

Recent advances in nanotechnology-enabled biosensors for detection of exosomes as new cancer liquid biopsy

Chang-Chieh Hsu  and Yun Wu 

Department of Biomedical Engineering, University at Buffalo, The State University of New York, Buffalo, NY 14260, USA
Corresponding author: Yun Wu. Email: ywu32@buffalo.edu

Impact Statement

Exosomes (also known as small extracellular vesicles) play important roles in cancer initiation, progression, metastasis, and drug resistance, and therefore, exosomes have emerged as promising biomarkers for cancer liquid biopsy. Conventional exosome characterization methods such as qRT-PCR and ELISA are limited by low sensitivity, tedious process, large sample volume, and high cost. Developing new biosensors to offer sensitive, simple, fast, low sample consumption, and cost-effective detection of exosomal biomarkers addresses an urgent need in the field of cancer liquid biopsy. We summarized recent advances in nanotechnology-enabled biosensors that detect exosomal RNAs and proteins for cancer screening, diagnosis, and prognosis. This review provides useful information for readers who are interested in exosome-based cancer liquid biopsy and bionanotechnologies.

Abstract

Cancer liquid biopsy detects circulating biomarkers in body fluids, provides information that complements medical imaging and tissue biopsy, allows sequential monitoring of cancer development, and, therefore, has shown great promise in cancer screening, diagnosis, and prognosis. Exosomes (also known as small extracellular vesicles) are cell-secreted, nanosized vesicles that transport biomolecules such as proteins and RNAs for intercellular communication. Exosomes are actively involved in cancer development and progression and have become promising circulating biomarkers for cancer liquid biopsy. Conventional exosome characterization methods such as quantitative reverse transcription polymerase chain reaction (qRT-PCR) and enzyme-linked immunosorbent assay (ELISA) are limited by low sensitivity, tedious process, large sample volume, and high cost. To overcome these challenges, new biosensors have been developed to offer sensitive, simple, fast, high throughput, low sample consumption, and cost-effective detection of exosomal biomarkers. In this review, we summarized recent advances in nanotechnology-enabled biosensors that detect exosomal RNAs (both microRNAs and mRNAs) and proteins for cancer screening, diagnosis, and prognosis. The biosensors were grouped based on their sensing mechanisms, including fluorescence-based biosensors, colorimetric biosensors, electrical/electrochemical biosensors, plasmonics-based biosensors, surface-enhanced

Raman spectroscopy (SERS)-based biosensors, and inductively coupled plasma mass spectrometry (ICP-MS) and photothermal biosensors. The future directions for the development of exosome-based biosensors were discussed.

Keywords: Exosomes, extracellular vesicles, biosensors, protein, microRNA, mRNA, cancer liquid biopsy

Experimental Biology and Medicine 2022; 247: 2152–2172. DOI: 10.1177/15353702221110813

Introduction

Cancer is one of the leading causes of death worldwide. It is estimated that there will be 27.5 million new cases and 16.5 million cancer deaths per year by 2040. Effective tests for cancer early detection, treatment response monitoring, and prognosis will greatly improve the patient outcome and reduce mortality. Liquid biopsy detects circulating cancer biomarkers in body fluids, such as blood, urine, and saliva. It is a non-invasive or minimally invasive test, provides additional information to complement medical imaging and tissue biopsy, allows sequential monitoring of cancer development, and, therefore, has shown great promise in cancer screening, diagnosis, precision medicine, treatment response evaluation, and prognosis.^{1,2} Unfortunately, current circulating biomarkers, such as carcinoembryonic

antigen (CEA) and prostate-specific antigen (PSA), are not sensitive and specific, and thus have limited diagnostic value.

Recently, exosomes (also known as small extracellular vesicles) have received wide attention as a new type of biomarker for cancer diagnosis. Exosomes are nanovesicles (40–160 nm) secreted by cells into extracellular environments.³ The generation of exosomes starts with the inward budding of cell membrane to form intraluminal vesicles (ILVs) in early endosomes, which then become multivesicular bodies (MVBs). MVBs fuse with the cell membrane and release exosomes (Figure 1). Exosomes exist in all types of body fluids, such as blood, urine, breast milk, ascites, and saliva. The major function of exosomes is to transfer biomolecules including proteins, DNAs, RNAs, and lipids from parent cells to recipient cells for cell–cell communication.

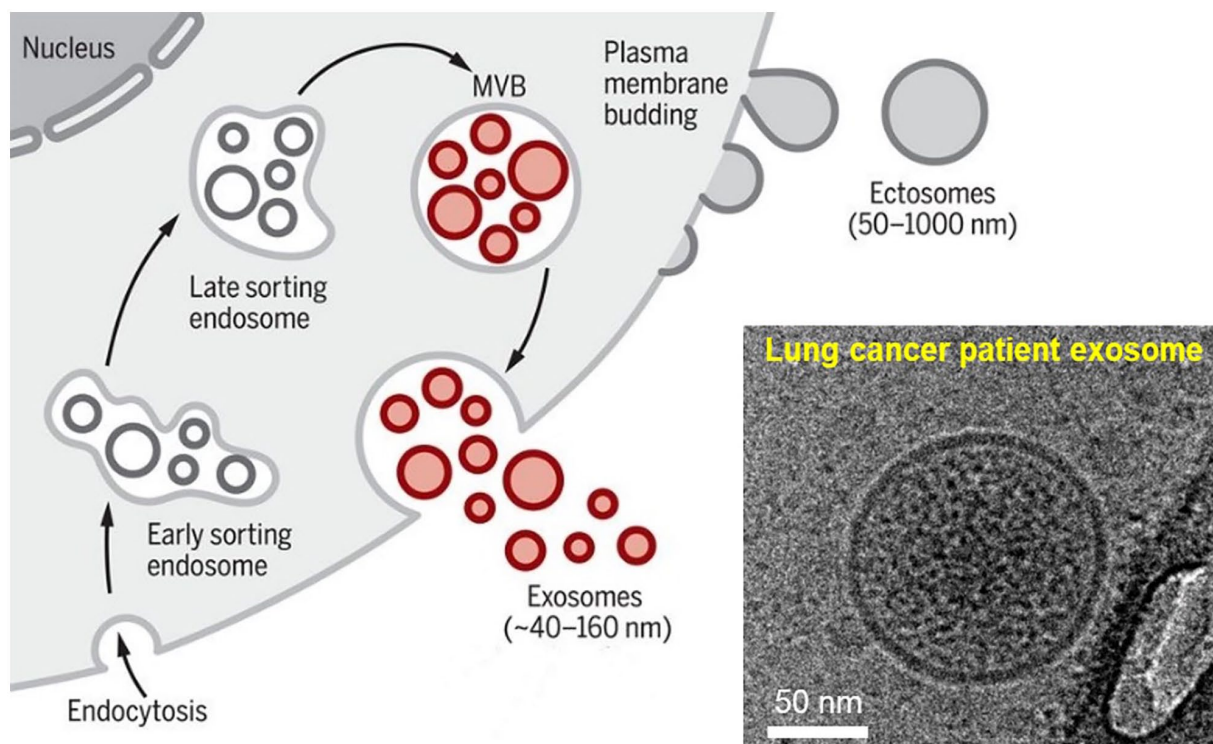


Figure 1. Exosome biogenesis and secretion. Exosomes are formed by inward budding of cell membrane to form intraluminal vesicles in early endosomes, which then develop into multivesicular bodies (MVB). MVB fuse with cell membrane and release exosomes. (Reprinted from Kalluri *et al.*³ ©2020 American Association for the Advancement of Science.) Inset: a CryoTEM image of an exosome in the blood of a lung cancer patient. (Reprinted from Wu *et al.*¹¹ ©2013 American Chemical Society.) (A color version of this figure is available in the online journal.)

Emerging evidence has indicated that exosomes actively participate in tumorigenesis and regulate tumor growth, angiogenesis, immune modulation, metastasis, and drug resistance, and therefore, they have become new and potent biomarkers for cancer liquid biopsy.^{4–6} Among various cargoes of exosomes, exosomal RNAs and proteins have been widely investigated as biomarkers for cancer liquid biopsy. Exosomal RNAs are typically quantified by conventional methods such as quantitative reverse transcription polymerase chain reaction (qRT-PCR), microarrays, and next-generation sequencing. The expression of exosomal proteins is usually measured by enzyme-linked immunosorbent assay (ELISA), western blotting, immunobead-based flow cytometry, and mass spectrometry. However, these techniques have low sensitivity and are tedious, labor-intensive, expensive, and time-consuming, which limit their clinical utility. To overcome these limitations, new biosensors have been developed as alternative technologies for exosome characterization. These biosensors offer sensitive, simple, fast, high throughput, and cost-effective detection of exosomal RNAs and proteins. For example, a lipid-polymer hybrid nanoparticles containing catalyzed hairpin DNA circuits (CLPHN-CHDC) biochip was 25-fold more sensitive than qRT-PCR in detecting exosomal glypican 1 (GPC1) mRNA for pancreatic cancer diagnosis.⁷ An immuno-cationic lipoplex nanoparticles (iCLN) biochip had 100-fold higher sensitivity than qRT-PCR in detecting miR-21 in epidermal growth factor receptor (EGFR) expressing exosomes for lung cancer diagnosis.⁸ Besides, the iCLN biochip required a lower sample volume (30 μ L versus 200 μ L) and had a much shorter assay time

(4 h versus 24 h). An exosome-templated nanoplasmonic assay and a surface-enhanced Raman spectroscopy (SERS)-based aptasensor offered >1000-fold and >500-fold higher sensitivity than ELISA in detecting exosomal EpCAM and exosomal CD63, respectively.^{9,10} Compared with conventional techniques, new biosensors typically consume small volume of samples and have miniaturized and compact design, which enable their quick adaptation to clinical settings. To date, many biosensors have demonstrated their great potential as cancer *in vitro* diagnostic tests. In this review, we introduce recent advances in nanotechnology-enabled biosensors that detect exosomal RNAs (Table 1) and proteins (Table 2) for cancer screening, diagnosis, and prognosis. The nanotechnology-enabled biosensors were categorized based on sensing mechanisms, including fluorescence-based biosensors, colorimetric biosensors, electrical/electrochemical biosensors, plasmonics-based biosensors, SERS-based biosensors, and inductively coupled plasma mass spectrometry (ICP-MS) and photothermal biosensors. Non-nanotechnology-enabled biosensors and technologies developed for exosome isolation and purification are not included in this review.

Nanotechnology-enabled biosensors for exosomal RNA detection

Fluorescence-based biosensors for exosomal RNA detection

Fluorescence-based biosensors offer highly sensitive, simple, and fast detection of exosomal RNAs, including both

Table 1. Nanotechnology-enabled biosensors for exosomal RNA detection.

Sensing mechanism	Biosensor Device	Disease	Biomarkers	Limit of Detection	Linear range	Assay time	Sample type	Sample volume	Exosome isolation	Exosome lysis	Ref.	
Fluorescence	Tethered cationic lipoplex nanoparticles (tCLN) biochip	Lung cancer	miR-21, TTF-1 mRNA	N/A	N/A	2 h	Serum	70 μ L	Yes	No	11	
	tCLN biochip	Lung cancer	miR-21, miR-25, miR-155, miR-210, and miR-486	N/A	N/A	2 h	Serum	60 μ L	Yes	No	12	
	tCLN biochip	Lung cancer	TTF-1 mRNA, TKTL-1 mRNA	N/A	N/A	2 h	Plasma	20 μ L	Yes	No	13	
	tCLN biochip	Liver cancer	AFP mRNA, GPC-3 mRNA	N/A	N/A	2 h	Plasma	20 μ L	Yes	No	14	
	tCLN biochip	Pancreatic cancer	miR-21, miR-10b, miR-212	N/A	N/A	2 h	Plasma	N/A	Yes	No	15	
	Tethered cationic lipid-polymer hybrid nanoparticles containing catalyzed hairpin DNA circuits (CLPHN-CHDC) biochip	Pancreatic cancer	GPC1 mRNA	5.755×10^4 exosomes/mL	10^5 – 10^8 exosomes/mL	2 h	Serum	10 μ L	No	No	7	
	tCLN biochip	Lung cancer	miR-21, PD-L1 mRNA, PD-L1 protein	N/A	N/A	6 h	Plasma	90 μ L	Yes	No	16	
	Microfluidic CLN (mCLN) biochip	Lung cancer	miR-21, TTF-1 mRNA	miR-21: 2.06×10^9 exosomes/mL; TTF-1 mRNA: 3.71×10^9 exosomes/mL	8×10^7 – 8×10^{10} exosomes/mL	10 min	Serum	30 μ L	Yes	No	17	
	Immuno-CLN (iCLN) biochip	Lung cancer	EGFR+ or PD-L1 + exosomal miR-21 and TTF-1 mRNA	10^6 exosomes/mL	10^6 – 10^{10} exosomes/mL	4 h	Serum	30 μ L	Yes	No	8	
	Split DNAzyme probe (SDP)	Melanoma, breast cancer, cervical cancer	miR-21	3.78×10^5 copies/mL	3×10^7 – 10^{10} exosomes/mL	~2 h	Serum	N/A	No	No	18	
	Nanoflares-based thermophoretic biosensor	Breast cancer	miR-375, miR-221, miR-210, miR-10b	0.36 fM	10^7 – 10^{10} exosomes/mL (miR-375: 0.17–170 fM)	2 h	Serum	0.5 μ L	Yes	No	19	
	Electrical and electrochemical	Ion-exchange nanomembrane-based electrical biosensor	Pancreatic cancer	miR-550	2 pM	2–200 pM	1.5 h	Cell-derived exosomes	100 μ L	Yes	No	20
		Tetraedral DNA nanolabel-based electrochemical (eTDN) biosensor	Breast cancer	miR-21	34 aM	100 aM–1 nM	>1 h	Plasma	500 μ L	Yes	Yes	21
		DNA strand displacement reaction (SDR)-based electrochemical biosensor	Breast cancer	miR-21	67 aM	N/A	>2 h	Serum	N/A	Yes	Yes	22
		DNA SDR-based paper electrochemical biosensor	Lung cancer	miR-155, miR-21	miR-155: 33.4 aM miR-21: 23.1 aM	1 fM–0.4 μ M	2 h	Plasma	N/A	Yes	Yes	23
		Localized surface plasmon resonance (LSPR)-based nanoplasmonic biosensor	Pancreatic cancer	miR-10b	83.2 aM	N/A	>12 h	Plasma	500 μ L	Yes	Yes	24
	SERS	Surface plasmon resonance imaging (SPRI)-based biosensor	Lung cancer	miR-21, miR-139, miR-200, miR-378	1.68 fM	2 fM–20 nM	~4 h	Plasma	N/A	Yes	Yes	25
Fe ₃ O ₄ @Ag-SERS tags-based dual-SERS biosensor		Pancreatic cancer	miR-10b	1 aM	2 aM–100 pM	>1 h	Plasma	N/A	Yes	Yes	26	
Plasmonic head-flocked gold nanopillar-based SERS biosensor		Breast cancer	miR-21, miR-222, miR-200c	1 aM	1 aM–100 pM	>20 h	Cell-derived exosomes	N/A	Yes	Yes	27	

TTF: thyroid transcription factor; TKTL: transketolase; AFP: alphafetoprotein; GPC: glypican; CLPHN-CHDC: cationic lipid-polymer hybrid nanoparticles-catalyzed hairpin DNA circuits; PD-L: programmed death-ligand; CLN: cationic lipoplex nanoparticles; EGFR: epidermal growth factor receptor; SDP: split DNAzyme probe; SDR: strand displacement reaction; SERS: surface-enhanced Raman spectroscopy.

Table 2. Nanotechnology-enabled biosensors for exosomal protein detection.

Sensing mechanism	Biosensor Device	Disease	Biomarkers	Limit of Detection	Linear range	Assay time	Sample type	Sample volume	Exosome isolation	Exosome lysis	Ref.
Fluorescence	Homogeneous, low-volume, efficient, and sensitive exosomal programmed death-ligand 1 (PD-L1) detection assay (HOLMES-Exo _{PD-L1})	Urothelial carcinoma; gastric carcinoma; prostate cancer; small cell lung cancer; ovarian sarcoma	PD-L1	17.6 pg/mL	0–353.8 pg/mL	N/A	Plasma	1 mL	Yes	No	28
	Exosome-oriented, aptamer nanoprobe-based profiling (ExoAPP) assay	Prostate cancer	CD63, EpCAM, and PSMA	1.6×10^5 exosomes/mL	1.6×10^5 – 1.6×10^8 exosomes/mL	~30 min	Serum	10 μ L	No	No	29
	Quantum dot (QD) FRET-based aptasensor	Breast cancer, lung cancer, liver cancer, thymic carcinoma	EpCAM	13 exosomes/mL	5×10^2 – 5×10^8 exosomes/mL	~1 h	Serum	200 μ L	No	No	30
	QD/photonic crystals-based assay	Pancreatic cancer	GPC1	5×10^8 exosomes/mL	10^7 – 10^9 exosomes/mL	~1.5 h	Cell-derived exosomes	N/A	Yes	No	31
	Homogeneous magneto-fluorescent exosome (hMFEX) nanosensor	Breast cancer	GPC1	6.56×10^7 exosomes/mL	7.8×10^7 – 3.9×10^{12} exosomes/mL	~2 h	Plasma	80 μ L	No	No	32
	DNA hybridization chain reaction–based aptasensor	Liver cancer	CD63	100 exosomes/mL	10^3 – 10^7 exosomes/mL	N/A	Serum	50 μ L	Yes	No	33
	Branched rolling circle amplification (BRCA)-based aptasensor	Gastric cancer	MUC1	4.27×10^4 exosomes/mL	10^5 – 10^8 exosomes/mL	>8 h	Plasma	N/A	Yes	No	34
	Enzyme-powered DNA motors–based aptasensor	Breast cancer	CD63	8.2×10^3 exosomes/mL	2×10^4 – 2×10^9 exosomes/mL	~3 h	Serum	N/A	No	No	35
	Catalytic hairpin DNA cascade reaction (HDCR)-based aptasensor	Liver cancer	CD63	1.16×10^6 exosomes/mL	1.75×10^6 – 7×10^9 exosomes/mL	>4 h	Cell-derived exosomes	200 μ L	Yes	No	36
	Nano-interfaced microfluidic exosome (nano-IMEX) biosensor	Ovarian cancer	CD9, CD81, EpCAM	5×10^4 exosomes/mL	10^6 – 10^{10} exosomes/mL	N/A	Plasma	2 μ L	No	No	37
	3D-nanopatterned herringbone (nano-HB) microfluidic device	Ovarian cancer	CD24, EpCAM, FR α	10^4 exosomes/mL	10^5 – 10^9 exosomes/mL	>2 h	Plasma	2 μ L	No	No	38
Colorimetric	Single-walled carbon nanotube (SWCNT)-based aptasensor	Breast cancer	CD63	5.2×10^8 exosomes/mL	1.84×10^9 – 2.21×10^{10} exosomes/mL	~40 min	Cell-derived exosomes	N/A	yes	no	39
Electrical and electrochemical	DNA nanotetrahedron (NTH)-based aptasensor	Liver cancer	N/A	2.09×10^4 exosomes/mL	10^5 – 10^{12} exosomes/mL	30 min	Cell-derived exosomes	10 μ L	Yes	No	40
	Magnetic bead–based aptasensor	Prostate cancer	PSMA	7×10^4 exosomes/mL	10^6 – 1.2×10^8 exosomes/mL	>5 h	Cell-derived exosomes	5 μ L	Yes	No	41
	Reduced graphene oxide (RGO)-based field-effect transistor (FET) biosensor	Prostate cancer	CD63	3.3×10^4 exosomes/mL	3.3×10^4 – 3.3×10^9 exosomes/mL	20 min	exosomes	10 μ L	Yes	No	42
	Graphene-based FET biosensor	Healthy donor	CD63	$\sim 5 \times 10^6$ exosomes/mL (0.1 μ g/mL)	N/A	~30 min	Plasma	10 μ L	Yes	No	43
	ZIF-8 metal-organic framework (MOF)-based electrochemical biosensor	Breast cancer	PD-L1	334 exosomes/mL	10^3 – 10^{10} exosomes/mL	>4 h	Serum	N/A	Yes	No	44
	UiO-66 MOF-based electrochemical biosensor	Brain cancer	EGFR, EGFRvIII	7.83×10^6 exosomes/mL	9.5×10^6 – 1.9×10^{10} exosomes/mL	>2 h	Serum	10 μ L	Yes	No	45

(Continued)

Table 2. (Continued)

Sensing mechanism	Biosensor Device	Disease	Biomarkers	Limit of Detection	Linear range	Assay time	Sample type	Sample volume	Exosome isolation	Exosome lysis	Ref.
Plasmonics	Nanoplasmonic exosome (nPLEX) biosensor	Ovarian cancer	CD24, EpCAM	3000 exosomes (670 aM)	N/A	30 min	Ascites	150 μ L	No	No	46
	Templated plasmonics for exosomes (TPEX) assay	Colorectal cancer and gastric cancer	CD63, CD24, EpCAM, MUC1	1500 exosomes	10^5 – 10^7 exosomes/mL	15 min	Ascites	1 μ L	No	No	9
SERS	SERS immunoassay	Breast cancer	CD63, HER2	~1200 exosomes (268 aM)	4.88×10^3 – 4.88×10^6 exosomes	~2 h	Cell culture medium	100 μ L	No	No	47
	SERS immunoassay	Lung cancer	PD-L1	1000 exosomes/mL	5×10^3 – 2×10^5 exosomes/mL	~40 min	Serum	4 μ L	Yes	No	48
	Multiplex SERS immunoassay	Pancreatic cancer, colorectal cancer, bladder cancer	GPC1, EpCAM, CD44 V6	2.3×10^6 exosomes/mL	N/A	2.5 h	Cell-derived exosomes	200 μ L	Yes	No	49
	Microarray-based SERS assay	Breast cancer	HER2, EpCAM, CD44, CD81, CD63, CD9	2×10^6 exosomes/mL (3.3 fM)	N/A	2 h	Plasma	15 μ L	Yes	No	50
	SERS-EpCAM aptasensor	Lung cancer	EpCAM	2.4×10^3 exosomes/mL	3.84×10^4 – 1×10^9 exosomes/mL	N/A	Plasma	100 μ L	No	No	10
	Hydrophobic assembled nanoacorn (HANA) platform-based SERS aptasensor	Breast cancer	CD63, EpCAM, HER2	50 exosomes/mL	10^5 – 10^9 exosomes/mL	>1 h	Plasma	15 μ L	No	no	51
	Triangular pyramidal DNA-Au nanoparticles-5,5'-dithiobis-(2-nitrobenzoic acid) (DTNB)-based SERS aptasensor	Breast cancer	EpCAM	1.1×10^5 exosomes/mL	10^6 – 10^{10} exosomes/mL	1.5 h	Plasma	10 μ L	Yes	No	52
	Gold-Silver-Silver core-shell-shell nanotrepangs (GSSNTs)-based SERS aptasensor	Breast cancer, prostate cancer, liver cancer	PSMA, HER2, AFP	PSMA: 2.6×10^4 exosomes/mL; HER2: 7.2×10^4 exosomes/mL; AFP: 3.5×10^4 exosomes/mL	10^3 – 10^7 exosomes/mL	~2 h	Serum	N/A	No	No	53
ICP-MS and Photothermal	$Fe_3O_4@MnO_2$ nanoflowers based ICP-MS and photothermal assay	Pancreatic cancer	GPC1	19.1 exosomes/mL	ICP-MS: 45 – 4.5×10^6 exosomes/mL; photothermal: 2.5×10^8 ~ 4.5×10^9 exosomes/mL	>5 h 20 min	Serum	~2 mL	Yes	No	54

AFP: alpha-fetoprotein; GPC: glypican; PD-L: programmed death-ligand; EGFR: epidermal growth factor receptor; SERS: Surface-enhanced Raman spectroscopy; PSMA: prostate-specific membrane antigen; QD: quantum dot; FRET: fluorescence resonance energy transfer; MUC: Mucin; RGO: reduced graphene oxide; FEI: field effect transistor; MOF: metal-organic frameworks; TPEX: templated plasmonics for exosomes; ICP-MS: inductively coupled plasma mass spectrometry.

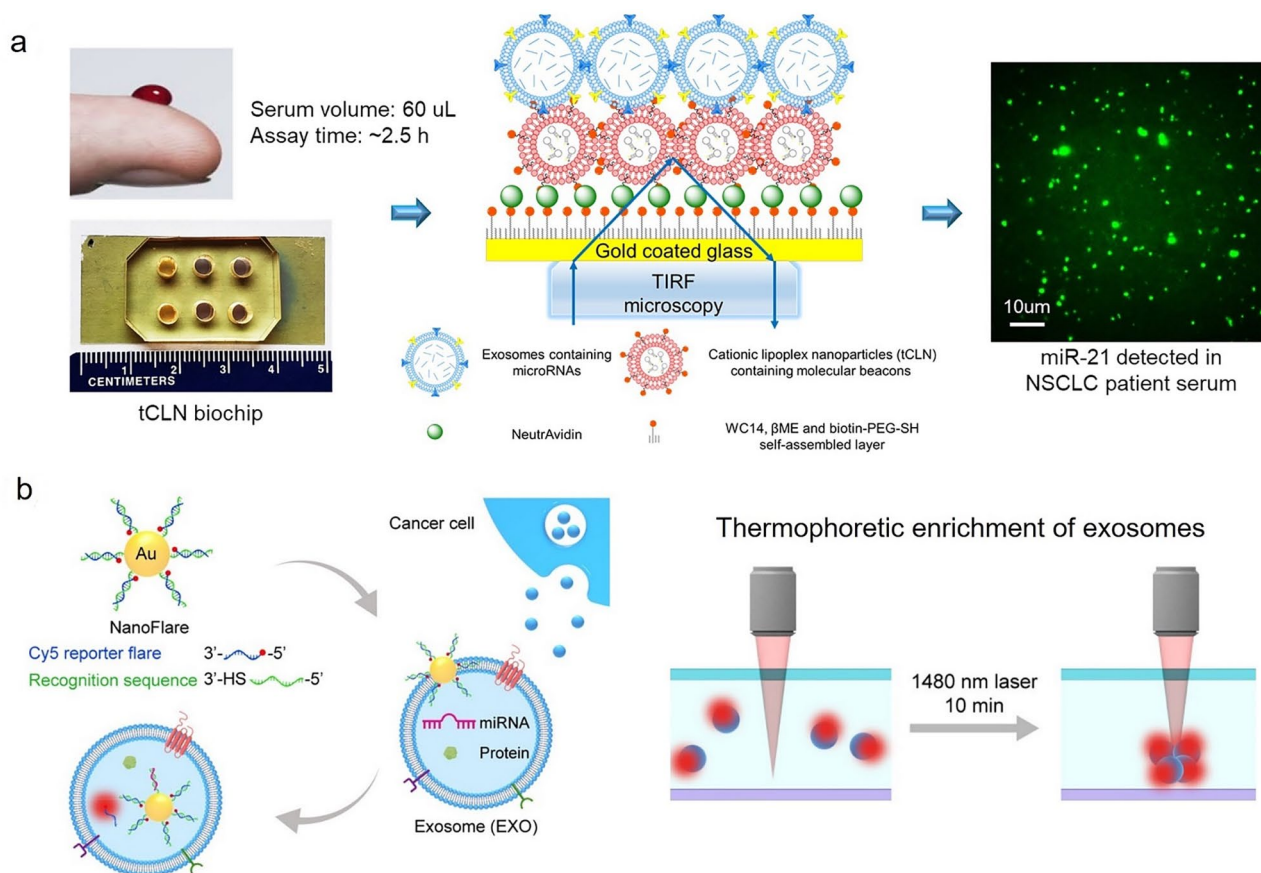


Figure 2. Sensing mechanisms of two representative fluorescence-based biosensors for exosomal RNA detection. (a) Sensing mechanism of tethered cationic lipoplex nanoparticles (tCLN) biochip in detecting exosomal RNAs. tCLN captured exosomes through electrostatic interaction. The fusion of exosomes with tCLN allowed the binding between molecular beacons and exosomal RNAs and thus restored the fluorescence signals from molecular beacons, which were detected by the total internal reflection fluorescence (TIRF) microscopy. (Reprinted from Liu *et al.*¹² ©2020 Frontiers.) (b) Sensing mechanism of nanoflares-based thermophoretic biosensor in detecting exosomal RNAs. After nanoflares were internalized inside exosomes, the hybridization of recognition sequences with target microRNAs released Cy5 reporter flare and restored fluorescence signals. Then laser irradiation was applied to enable thermophoretic enrichment of exosomes to amplify fluorescence signals. (Reprinted from Zhao *et al.*¹⁹ ©2020 American Chemical Society.) (A color version of this figure is available in the online journal.)

mRNAs and microRNAs (miRs), for cancer diagnosis. We developed a tethered cationic lipoplex nanoparticles (tCLN) biochip to capture exosomes and in situ detect exosomal RNAs for lung cancer diagnosis (Figure 2(a)).¹¹ In the tCLN biochip, molecular beacons (MBs), which are sensing probes for RNAs, were encapsulated within the CLN and tethered to the biochip surface. The positively charged tCLN captured negatively charged exosomes through electrostatic interaction. The CLN-exosome fusion led to the binding of MBs to target RNAs, which restored the fluorescence signals from MBs. These fluorescence signals were recorded by total internal reflection fluorescence (TIRF) microscopy and converted to the levels of exosomal RNAs. The tCLN biochip detected significant differences in the levels of exosomal miR-21, miR-25, miR-155, miR-210, and miR-486 in serum samples from lung cancer patients ($n=71$) than normal controls ($n=17$).^{11,12} The tCLN assay also detected significantly higher levels of exosomal thyroid transcription factor 1 (TTF-1) mRNA and transketolase 1 (TKTL-1) mRNA in plasma samples from lung cancer patients ($n=78$) than those from healthy controls ($n=40$) and patients with benign lung nodules ($n=38$).¹³ Using exosomal alphafetoprotein (AFP) mRNA and glypican 3 (GPC3) mRNA as the biomarkers,

the tCLN assay distinguished liver cancer patients ($n=40$) from normal controls ($n=38$) with an accuracy of 99.5%.¹⁴ With exosomal miR-21 and miR-10b as biomarkers, the tCLN assay differentiated pancreatic cancer patients ($n=36$) from normal controls ($n=65$) with an accuracy of 79.1%.¹⁵

We and others have further developed the tCLN assay to improve its sensing performances.^{7,16,17} Hu *et al.*⁷ developed a CLPHN-CHDC biochip in which cationic lipid-polymer hybrid nanoparticles (CLPHN) replaced CLN, and two catalyzed hairpin DNA circuits (CHDC) replaced MBs to achieve signal amplification and thus allow for the quantification of RNAs with low copy numbers. Using exosomal GPC1 mRNA as the biomarker, the CLPHN-CHDC biochip identified pancreatic cancer patients ($n=118$) from healthy controls ($n=60$) and patients with benign pancreatic disease ($n=15$) with 100% accuracy. The CLPHN-CHDC biochip offered 25-fold higher sensitivity than qRT-PCR. Zhou *et al.*¹⁶ developed a high-throughput tCLN assay to process up to 384 samples per assay. Besides, after the measurement of exosomal RNAs was completed, fluorescent dye AF-647 labeled programmed death ligand-1 (PD-L1) antibodies were applied to detect exosomal PD-L1 expression, enabling the simultaneous detection of exosomal RNAs and proteins. A deep learning

algorithm was used to perform image analysis and quantify the expression of exosomal biomarkers from each individual exosome. Significantly higher levels of exosomal PD-L1 mRNA, miR-21 and PD-L1 protein were observed in plasma samples from lung cancer patients ($n=34$) than normal controls ($n=35$). To further improve the detection efficiency of the tCLN assay, we developed a microfluidic CLN (mCLN) assay to realize ultrafast detection of exosomal RNAs for lung cancer diagnosis.¹⁷ In the mCLN assay, a micromixer biochip was used to effectively mix exosomes and CLN, which facilitated the fusion between exosomes and CLN and enabled the detection of exosomal RNAs in 10 min. The mCLN assay detected significantly higher expression of exosomal miR-21 and TTF-1 mRNA in serum samples from lung cancer patients ($n=10$) than normal controls ($n=5$).

Since all cells release exosomes, capturing tumor-derived exosomes (TEXs) from all other exosomes and detecting TEX biomarkers improve the sensitivity and specificity of cancer diagnosis. To achieve this goal, we advanced the tCLN biochip to the second generation, the immuno-CLN (iCLN) biochip.⁸ In the iCLN biochip, antibodies against tumor associated proteins such as EGFR and PD-L1 were immobilized on the biochip surface to capture TEXs that express EGFR and PD-L1. Then, CLN containing molecular beacons were applied to detect TEX miR-21 and TTF-1 mRNA. The limit of detection (LOD) of iCLN biochip was 10^6 exosomes/mL, which was 100-fold higher than qRT-PCR. The iCLN biochip detected significantly higher levels of EGFR-expressing exosomal miR-21/TTF-1 mRNA and PD-L1-expressing exosomal miR-21/TTF-1 mRNA in serum samples from lung cancer patients ($n=20$) than normal controls ($n=10$), diagnosing lung cancer with 100% accuracy.

He *et al.*¹⁸ developed a DNA nanotechnology-based single exosome imaging assay. In this assay, a split DNAzyme probe (SDP) was used for exosomal miR-21 detection. The SDP consisted of two inactive DNAzymes and a ribonucleobase-modified molecular beacon as the substrate for the DNAzymes. With streptolysin O treatment, the SDP entered exosomes and was activated by its hybridization with target miR-21. The activated SDP catalyzed the cleavage of the molecular beacon in the presence of Mg^{2+} ions. Strong fluorescence signals were thus generated and captured by TIRF microscopy. Single exosome analysis was then performed to measure exosomal miR-21 expression. The LOD of this assay was 378 copies/ μ L, and the linear range was from 3×10^7 to 10^{10} exosomes/mL. Higher levels of exosomal miR-21 were detected in serum samples from melanoma ($n=3$), breast cancer ($n=3$), and cervical cancer ($n=3$) patients compared with normal controls ($n=3$). Reduced exosomal miR-21 levels were observed in the serum samples of these patients after the clinical treatment. These results demonstrate the potential clinical utility of this single exosome imaging assay in cancer diagnosis and treatment response monitoring.

Zhao *et al.*¹⁹ reported a nanoflares-based thermophoretic biosensor to detect exosomal microRNAs for breast cancer diagnosis (Figure 2(b)). In this assay, nanoflares were first prepared by modifying gold nanoparticles with Cy5-labeled DNA reporter sequences and recognition sequences that are complementary to target microRNAs. After the nanoflares diffused into exosomes, the hybridization of microRNAs

with recognition sequences released Cy5-DNA reporter sequences from the gold nanoparticles and thus restored Cy5 fluorescence signals. Localized laser irradiation was then used to thermophoretically enrich exosomes labeled with nanoflares to amplify the fluorescence signals for sensitive detection of exosomal microRNAs. The LOD of this assay was 0.36 fM and the linear range was from 0.17 to 170 fM. The expression of a panel of four exosomal microRNAs (miR-375, miR-221, miR-210, and miR-10b) was measured in serum samples from breast cancer patients ($n=17$) and normal controls ($n=12$). Among these biomarkers, exosomal miR-375 showed the highest diagnostic accuracy (90%) in detecting breast cancer.

Electrical and electrochemical biosensors for exosomal RNA detection

With the miniaturization of electrodes and the incorporation of nanotechnologies, electrical and electrochemical biosensors have emerged as potent *in vitro* diagnostics for cancer. Taller *et al.*²⁰ developed an ion-exchange nanomembrane-based electrical biosensor that enabled exosome on-chip lysis and exosomal microRNA detection. Exosomes were first lysed through the application of surface acoustic waves. The released exosomal RNAs were driven through the pores of an ion-exchange nanomembrane by an electric field. To realize the exosomal miR-550 detection, sensing probes were functionalized on the surface of an ion-exchange nanomembrane. The capture of miR-550 changed the current-voltage characteristic dramatically and allowed the quantification of miR-550 expression. The LOD of this assay in detecting exosomal miR-550 from PANC1 pancreatic cancer cells was 2 pM with two decades of linear range. It was found that the concentration of miR-550 in PANC1 exosomes was 13 pM, that is, ~ 14 copies of miR-550 per exosome.

DNA nanotechnologies have been integrated with electrochemical sensing for exosomal microRNA detection. Liu *et al.*²¹ developed a tetrahedral DNA nanolabel-based electrochemical (eTDN) sensor for exosomal miR-21 detection. The TDN first partially hybridized with miR-21, and then hybridized with peptide nucleic acid (PNA) probes on the gold electrode surface to form TDN-miR-PNA complexes. In the presence of RuHex cations, electrochemical signals were measured to quantify the expression of miR-21. The eTDN sensor showed LOD of ~ 34 aM and the linear range of 100 aM to 1 nM. It detected significantly higher expression of exosomal miR-21 in 500 μ L plasma samples from breast cancer patients ($n=10$) than normal controls ($n=10$). Zhang *et al.*²² and Yang *et al.*²³ developed DNA strand displacement reaction (SDR)-based electrochemical sensors to detect exosomal microRNAs. In the electrochemical biosensor developed by Zhang *et al.*,²² as shown in Figure 3, the DNA walkers first partially hybridized with the capture probes (L-Cp) immobilized on magnetic beads to form DNA walker-L-Cp-magnetic bead complexes. The addition of miR-21 initiated DNA SDR and released DNA walkers. After magnetic separation, the DNA walkers were applied to the DNA tracks, which were built by immobilizing methylene blue-modified hairpin probes 1 (MB-H1) on a gold electrode. After the DNA walkers hybridized with the

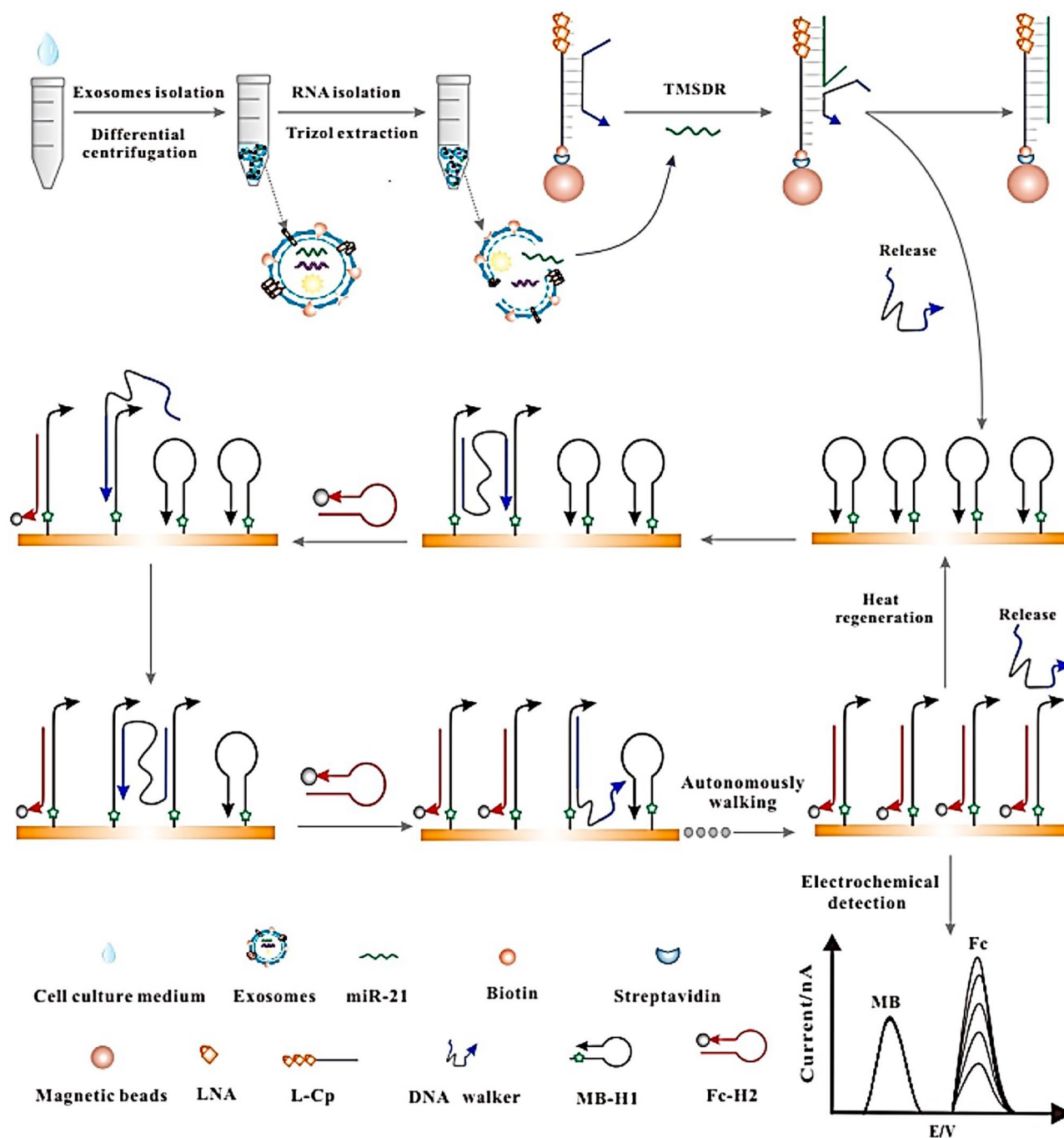


Figure 3. Sensing mechanism of the DNA strand displacement reaction–based electrochemical biosensor in detecting exosomal miR-21 for breast cancer diagnosis. miR-21 was extracted from exosomes isolated from serum. Locked nucleic acid–modified capture probes (L-Cp) were conjugated on the surface of magnetic beads. DNA walkers partially hybridized to L-Cp to form DNA walker-L-Cp-magnetic bead complexes. In the presence of miR-21, L-Cp hybridized with miR-21 and the DNA walkers were released into the solutions. DNA walkers were then extracted using magnetic separation and applied to DNA tracks, which were made from gold electrodes. After DNA walkers bound to MB-H1 probes immobilized on the surface, Fc-H2 probes were added to hybridize with MB-H1 probes and initiate the walking of DNA walkers along the track. The approach of Fc-H2 probes to the surface led to the increase of electrochemical signals from Fc. The electrochemical signal ratio of Fc and MB was measured and used to characterize the expression of exosomal miR-21. (Reprinted from Zhang *et al.*²² ©2017 Elsevier B.V.) (A color version of this figure is available in the online journal.)

MB-H1, ferrocene-labeled hairpin probes 2 (Fc-H2) were added to hybridize with MB-H1 through DNA SDR and initiate the walking of DNA walkers along the DNA tracks. The hybridization of Fc-H2 with MB-H1 brought ferrocene close to the surface of the gold electrode, and thus generated detectable electrochemical signals. This biosensor measured electrochemical signal ratios of ferrocene and methylene

blue (reference), which were converted to the expression of exosomal miR-21. The LOD for miR-21 detection was 67 aM. The biosensor was regenerative, offering stable sensing performance for at least 5 cycles. The biosensor detected 2.5-fold higher levels of exosomal miR-21 in serum samples from breast cancer patients than normal controls, demonstrating its potential clinical applications in breast cancer diagnosis.

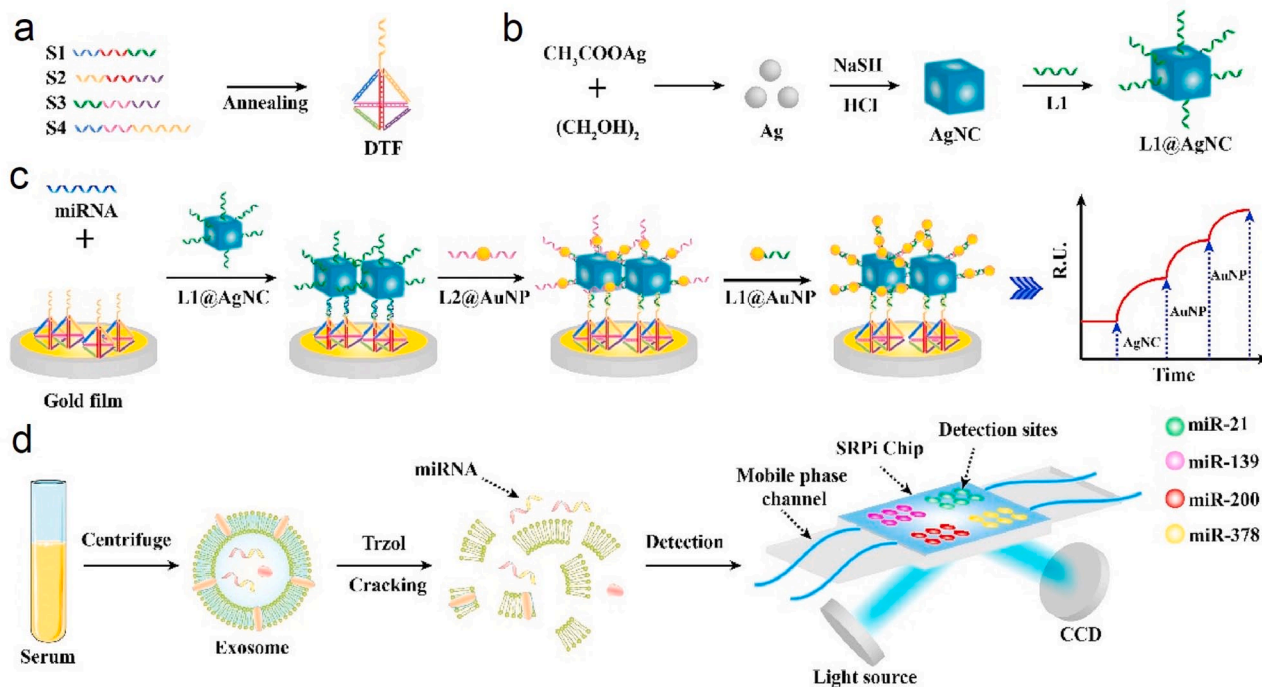


Figure 4. Sensing mechanism of a surface plasmon resonance imaging (SPRI) biosensor for multiplex detection of exosomal microRNAs. (a) A DNA tetrahedral framework (DTF) was prepared by self-assembly and attached to the surface of the SPRI biochip. (b) Single-strand DNA L1-modified silver nanocubes (L1@AgNC) were prepared. (c) MicroRNA and L1@AgNC are then applied onto the SPRI biochip to form DNA DTF-microRNA-AgNC complexes. Finally, single-strand DNA L2-modified gold nanoparticles (L2@AuNP) and single-strand DNA L1-modified gold nanoparticles (L1@AuNP) were sequentially added to form Au-on-Ag heterostructures, which amplified the SPR signals for sensitive detection of microRNA targets. (d) The workflow of SPRI assay. Exosomes were isolated from serum samples via centrifugation. Trizol was used to extract microRNAs from exosomes. The expression of microRNAs was measured by the SPRI assay. (Reprinted from Wu *et al.*²⁵ ©2020 Elsevier B.V.) (A color version of this figure is available in the online journal.)

In the electrochemical sensor developed by Yang *et al.*,²³ the electrode was prepared by depositing gold nanoparticles on the graphene-coated conductive carbon fiber paper, which provided a large, three-dimensional, and highly sensitive sensing surface. Hairpin DNA capture probes were conjugated on the surface of the electrode to capture microRNA targets. After the hybridization of microRNA targets with hairpin DNA capture probes, a Zr metal-organic framework (Zr-MOF) loaded with DNA detection probes (complementary to capture probes) and electroactive dyes was added to initiate DNA SDR and generate electrochemical signals. This paper-based electrochemical sensor simultaneously detected exosomal miR-155 and miR-21 with an LOD of 33.4 aM and 23.1 aM, respectively. The linear range of this assay was 1 fM to 0.4 μ M. Significantly higher levels of exosomal miR-155 and miR-21 were detected in plasma samples from lung cancer patients ($n=8$) than normal controls ($n=5$), demonstrating the feasibility of this electrochemical sensor in lung cancer diagnosis.

Plasmonic-based biosensors for exosomal RNA detection

Plasmonic sensors are highly sensitive and label-free approaches for the detection of exosomal microRNAs. A localized surface plasmon resonance (LSPR)-based nanoplasmonic biosensor was developed by Joshi *et al.*²⁴ to detect exosomal miR-10b for pancreatic cancer diagnosis. Gold nanoprisms with ~40 nm edge length were first covalently bound

on the surface of a salinized glass substrate. Then the surface of gold nanoprisms was functionalized with single-stranded DNAs (ssDNAs) complementary to miR-10b. The binding of miR-10b to ssDNAs formed DNA duplexes, which increased the local refractive index and shifted the LSPR dipole peak to higher wavelengths. The wavelength shift was measured and converted to the expression of miR-10b. The LOD of the biosensor was 83.2 aM. The biosensor was regenerative and provided uncompromised detection sensitivity for at least five hybridization/de-hybridization cycles of miR-10b over a 5-day period. The biosensor detected significantly higher expression of miR-10b in exosomes from patients with pancreatic ductal adenocarcinoma ($n=3$) than those from normal controls ($n=3$) and chronic pancreatitis patients ($n=3$), providing a new approach for pancreatic cancer diagnosis.

Wu *et al.*²⁵ developed a surface plasmon resonance imaging (SPRI)-based biosensor for multiplex detection of exosomal microRNAs for lung cancer diagnosis. As shown in Figure 4, a DNA tetrahedral framework (DTF) was assembled and attached to the surface of the SPRI biochip. Exosomal microRNAs were captured by ssDNAs modified on the surface of silver nanocubes (AgNC). Then the microRNA-AgNC complexes were applied on the SPRI biochip to interact with DNA DTF and form DNA DTF-microRNA-AgNC complexes. Finally, gold nanoparticles were added to form Au-on-Ag heterostructures, which amplified the SPR signals for sensitive detection of microRNA targets. The SPRI biosensor had an LOD of 1.68 fM and a linear range of 2 fM to 20 nM. Significantly higher levels of exosomal miR-21,

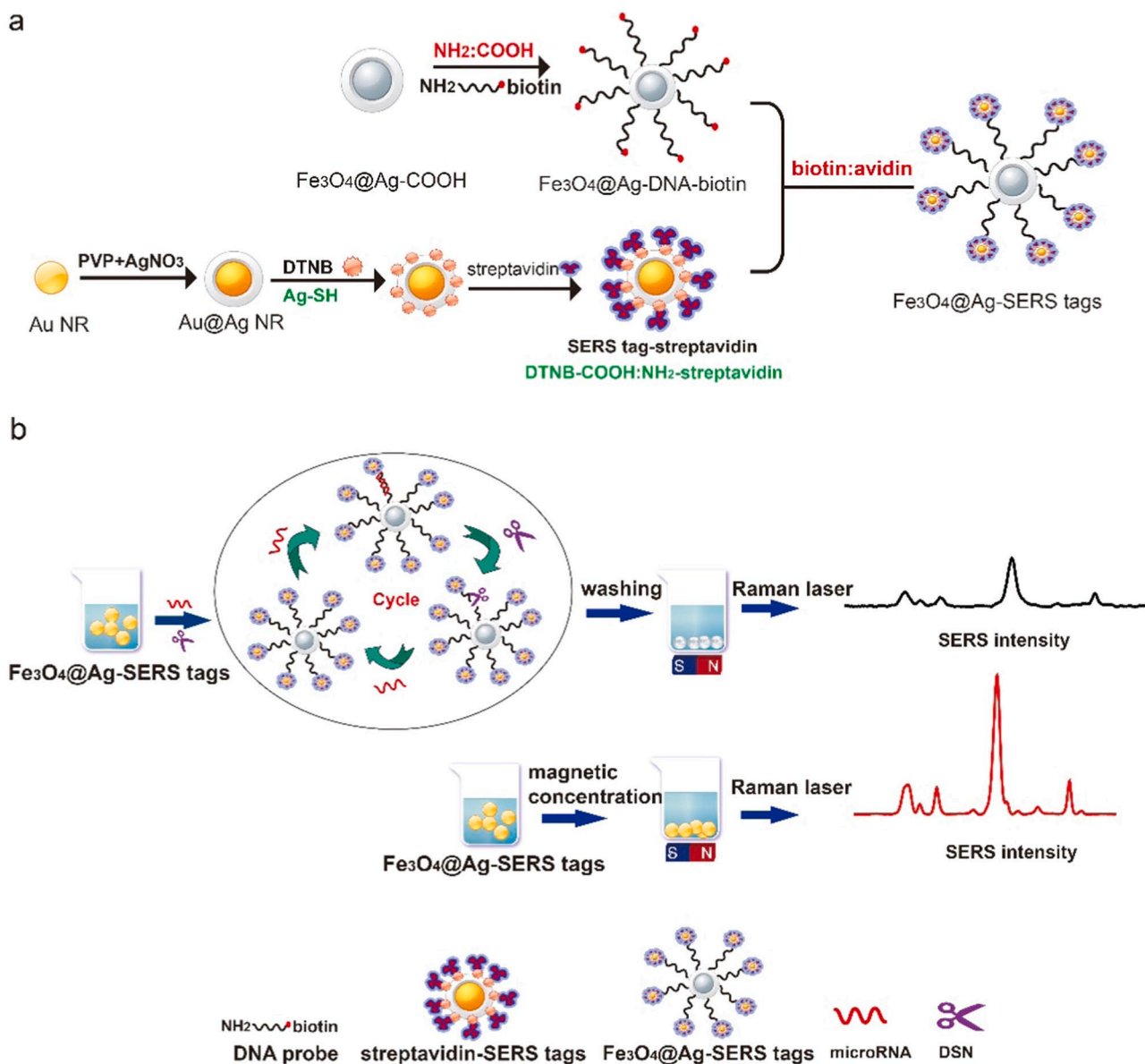


Figure 5. Sensing mechanism of dual-SERS biosensor for exosomal miR-10b detection for pancreatic cancer diagnosis. (a) $\text{Fe}_3\text{O}_4@Ag\text{-SERS tags}$ were prepared by conjugating $\text{Fe}_3\text{O}_4@Ag\text{-DNA-biotin}$ with SERS-tag-streptavidin (i.e. $\text{Au}@Ag@DTNB\text{-streptavidin}$). (b) In the presence of miR-10b and duplex-specific nuclease (DSN), SERS tags were continuously cleaved from $\text{Fe}_3\text{O}_4@Ag$ and resulted in the reduction of SERS signals. (Reprinted from Pang *et al.*²⁶ ©2019 Elsevier B.V.) (A color version of this figure is available in the online journal.)

miR-378, miR-200, and miR-139 were detected in plasma samples from lung cancer patients ($n=5$) than normal controls ($n=5$), demonstrating the potential application of the SPRi biosensor in lung cancer diagnosis.

SERS-based biosensors for exosomal RNA detection

SERS offers molecular fingerprint specificity and high sensitivity, making it an attractive approach to detect a trace amount of exosomal microRNAs in complex clinical samples. Pang *et al.*²⁶ reported a dual-SERS biosensor for one-step and one-pot analysis of exosomal miR-10b for diagnosing pancreatic cancer (Figure 5). In this assay, $\text{Fe}_3\text{O}_4@Ag\text{-DNA}$ was first conjugated with SERS tags, that is, $\text{Au}@Ag@DTNB$ (5,5-dithiobis-2-nitrobenzoic acid) to prepare

$\text{Fe}_3\text{O}_4@Ag\text{-SERS tags}$. Exosomal miR-10b was then added to hybridize with the DNA probe of the $\text{Fe}_3\text{O}_4@Ag\text{-SERS tags}$. Then a duplex-specific nuclease (DSN) was added to cleave the DNA probe and release the SERS tags and miR-10b. The dissociation of SERS tags from $\text{Fe}_3\text{O}_4@Ag$ attenuated SERS signals. The released miR-10b could bind to the DNA probe of another $\text{Fe}_3\text{O}_4@Ag\text{-SERS tags}$ and the cycle could be repeated to enable signal amplification. The LOD of this assay was 1 aM and the linear range was 2 aM to 100 pM. Significantly higher levels of exosomal miR-10b were detected in plasma samples from patients with pancreatic ductal adenocarcinoma ($n=5$) than in chronic pancreatitis patients ($n=5$) and normal controls ($n=5$).

Lee *et al.*²⁷ developed an SERS biosensor based on plasmonic head-flocked gold nanopillars to detect exosomal microRNAs for breast cancer diagnosis. The surface of

head-flocked gold nanopillars was first modified with locked nucleic acid (LNA) capture probes. After the capture of exosomal microRNAs, Cy3-labeled LNA detection probes were added to form LNA capture probe/exosomal microRNA/Cy3-LNA detection probe complexes. The formation of such complexes reduced the gap between nanopillars to <10 nm, greatly increased the coupling of local surface plasmons, created sensing hot spots, and thus generated strong Cy3 signals. This assay detected miR-21, miR-222, and miR-200c in exosomes derived from multiple breast cancer cell lines corresponding to luminal (MCF-1, BT474), HER2+ (SKBR3, AU565), and triple-negative (MDA-MB-231 and HCC1143) subtypes. The LOD of this assay was 1 aM and the linear range was 1 aM to 100 pM.

Nanotechnology-enabled biosensors for exosomal protein detection

Fluorescence-based biosensors for exosomal protein detection

The fluorescence-based sensing mechanism is the most widely used strategy for the detection of exosomal proteins. Huang *et al.*²⁸ developed a homogeneous, low-volume, efficient, and sensitive exosomal programmed death-ligand 1 (PD-L1) detection assay (HOLMES-Exo_{PD-L1}) for cancer diagnosis. MJ5C aptamer, a small 33-nt hairpin DNA sequence, was first developed to offer high binding affinity with PD-L1 protein. After the capture of exosomes expressing PD-L1 by Cy5-labeled MJ5C aptamers, an infrared laser was shined on the sample to create a micrometer-sized temperature gradient. Thermophoresis was used to drive free aptamer away from the hot spot, and therefore, the fluorescent signals were mainly from exosome-aptamer complexes that remained in the hot spot. The HOLMES-Exo_{PD-L1} assay showed an LOD of 17.6 pg/mL, which was 11-fold higher than ELISA, and the linear range from 0 to 353.8 pg/mL. The HOLMES-Exo_{PD-L1} assay effectively distinguished cancer patients ($n=34$) from healthy controls ($n=22$) with high accuracy (area under the curve [AUC]=0.999).

Fluorescence quench and fluorescence resonance energy transfer (FRET) were utilized to improve detection sensitivity and specificity. Jin *et al.*²⁹ presented an exosome-oriented, aptamer nanoprobe-based profiling (ExoAPP) assay for exosome surface protein profiling. Quenched aptamer/graphene oxide nanoprobe were prepared by attaching fluorescent dye-labeled aptamers onto the graphene oxide surface. After the binding with exosomal protein targets, aptamers were released from the graphene oxide and their fluorescence signals were restored. Deoxyribonuclease I (DNase I) was used to cut the aptamers from the exosome surface to recycle exosomes and thus amplify the fluorescence signals. The LOD of the ExoAPP assay was 1.6×10^5 exosomes/mL, and the linear range was from 1.6×10^5 to 1.6×10^8 exosomes/mL. The protein profiling capability of the ExoAPP assay was demonstrated by detecting CD63, EpCAM, CEA, PTK-7, AFP, PSMA, and PDGF on exosomes from five cell lines, including HepG2, MCF-7, MCF-10A, SGC7901, and HeLa. The ExoAPP assay detected significantly higher levels of exosomal CD63, EpCAM, and PSMA levels

in serum samples from prostate cancer patients ($n=8$) than normal controls ($n=6$), demonstrating the feasibility of prostate cancer diagnosis. Zhu *et al.*³⁰ reported the quantum dot (QD) FRET-based aptasensor for exosomal EpCAM detection. QD, gold nanoparticles, and EpCAM aptamers were conjugated on Fe₃O₄ nanoparticles to generate the FRET nanoprobe. When EpCAM aptamers bound with exosomes, the FRET signal was turned on to allow the quantification of exosomal EpCAM expression. The LOD of this aptasensor was 13 exosomes/mL. Significantly higher levels of exosomal EpCAM were observed in serum samples from cancer patients ($n=12$, including lung cancer, breast cancer, liver cancer, and thymic carcinoma) than normal controls ($n=6$).

Various signal amplification methods have been applied to improve the sensitivity and specificity. Zhang *et al.*³¹ used photonic crystals to achieve fluorescent signal amplification. In this assay, quantum dots conjugated with GPC1 antibodies (anti-GPC1/QD) were used to label exosomes expressing GPC1. After the removal of free anti-GPC1/QD, the sample was applied to the biochip coated with photonic crystals to enable fluorescent signal amplification. This assay successfully detected the expression of GPC1 in exosomes derived from Panc-1 cells, demonstrating its potential application in pancreatic cancer diagnosis. The LOD of this assay was 5×10^8 exosomes/mL and the linear range was from 10^7 to 10^9 exosomes/mL.

DNA nanotechnologies have been applied to enable fluorescence signal amplification and thus allow sensitive detection of exosomal proteins. Li *et al.*³² developed a homogeneous magneto-fluorescent exosome (hMFEX) nanosensor for breast cancer diagnosis (Figure 6). In the hMFEX assay, exosomes expressing GPC1 were first captured by GPC1 antibody-functionalized magnetic beads. Extended CD63 aptamers were added to form magnetic bead-exosome-aptamer complexes. The complexes were then mixed with three DNA hairpins. The extended terminus of the CD63 aptamers served as the toehold to trigger the toehold-mediated strand displacement (TMSD) reaction among the DNA hairpins, which produced DNA three-way junctions (TWJs). Finally, tertiary amine-containing tetraphenylene (TPE-TA) and graphene oxide (GO) were introduced to generate fluorescence signals from DNA TWJs, which were converted to the expression of exosomal GPC1. The LOD of the hMFEX nanosensor was 6.56×10^7 exosomes/mL and the linear range was from 7.8×10^7 to 3.9×10^{12} exosomes/mL. Exosomal GPC1 measured by the hMFEX nanosensor distinguished breast cancer patients ($n=37$) from normal controls ($n=10$) with a sensitivity of 86.11%, specificity of 90%, and an AUC of 0.95.

Shi *et al.*³³ used a DNA hybridization chain reaction to amplify fluorescent signals from an aptasensor, enabling sensitive detection of exosomal CD63 for liver cancer diagnosis. The CD63 antibodies were first modified on the surface of magnetic nanoparticles to capture the exosomes. Then probe 1 consisted of a CD63 aptamer sequence and a trigger sequence was added to bind to the surface of exosomes via the CD63 aptamer sequence. The trigger sequence was then hybridized with two FAM-labeled probes (probes 2 and 3). This hybridization chain reaction generated strong fluorescence signals and allowed sensitive detection of exosomal

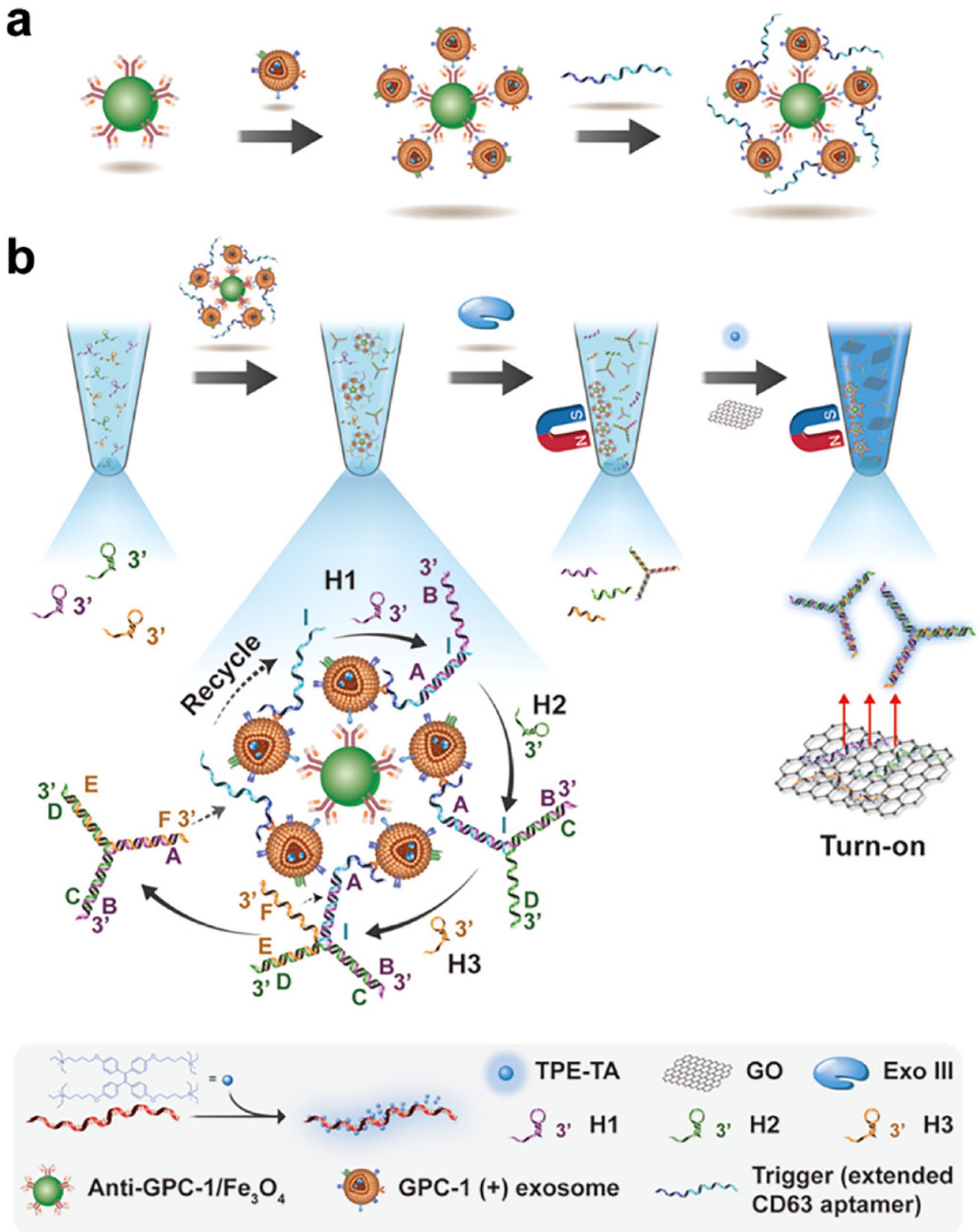


Figure 6. Sensing mechanism of the hMFEX nanosensor. (a) Exosomes expressing GPC1 were captured by GPC1 antibody conjugated magnetic beads and subsequently bound with extended CD63 aptamers, forming the magnetic bead-exosome-aptamer complexes. (b) The complexes were mixed with three DNA hairpins to trigger a toehold-mediated strand displacement (TMSD) reaction among the DNA hairpins and produced DNA three-way junctions (TWJs). Tertiary amine-containing tetraphenylene (TPE-TA) and graphene oxide (GO) were added to generate fluorescence signals from DNA TWJs, allowing the quantification of exosomal GPC1 expression. (Reprinted from Li *et al.*³² ©2020 American Chemical Society.) (A color version of this figure is available in the online journal.)

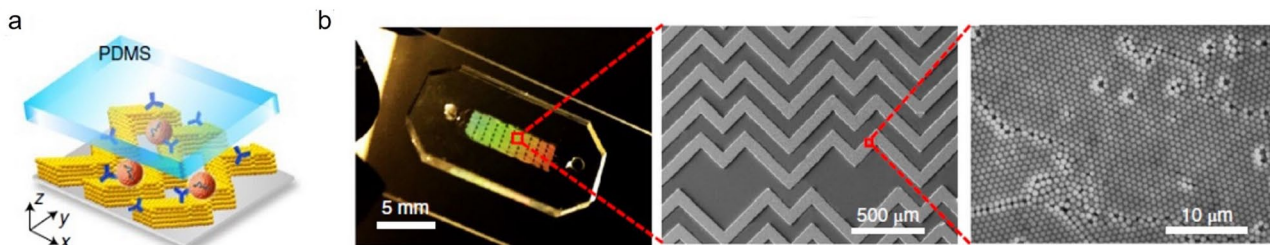


Figure 7. Sensing mechanism of a 3D-nanopatterned herringbone (nano-HB) microfluidic device. (a) Schematic of the 3D-nano-HB microfluidic device. Porous herringbone structures offered large surface area for antibody immobilization to enhance exosome capture efficiency. The expression of exosomal proteins was quantified by fluorogenic ELISA. (b) A nano-HB device fabricated with 960 nm silica colloids. (Reprinted from Zhang *et al.*³⁸ ©2019 Nature America, Inc.) (A color version of this figure is available in the online journal.)

CD63 with an LOD of 100 exosomes/mL and a linear range of 10^3 – 10^7 exosomes/mL. This assay detected higher exosomal CD63 levels in liver cancer patients ($n=6$) compared to normal controls ($n=8$).

Huang *et al.*³⁴ reported a branched rolling circle amplification (BRCA)-based aptasensor to detect exosomal Mucin 1 (MUC1) for gastric cancer diagnosis. Exosomes were first labeled with MUC1-aptamers. Then the MUC1-aptamer-exosome complexes were heated up to release MUC1-aptamers. A padlock probe partially complementary to MUC1-aptamer was added, and BRCA was started by adding the second primer. Finally, the amount of double-stranded DNA products was detected by SYBR green I fluorescent dye and converted to the expression of exosomal MUC1. This BRCA-based aptasensor detected higher exosomal MUC1 levels in plasma samples of gastric cancer patients ($n=10$) compared to normal controls ($n=12$). The LOD was 4.27×10^4 exosomes/mL and the linear range was from 10^5 to 10^9 exosomes/mL.

Yu *et al.*³⁵ utilized enzyme-powered DNA motors to amplify signals for the detection of exosomal CD63 in serum samples from breast cancer patients. Motor strands and FAM-labeled substrate strands were conjugated onto gold nanoparticles (GNP). CD63 aptamers were used as the locking strands to silence the motor strands. In the presence of exosomes, CD63 aptamers bound to exosomes and dissociated from the GNP, and the motor strands were thus activated. The activated motor strands hybridized with substrate strands, generating recognition sites that were recognized by the nicking endonuclease. After the cleavage of substrate strands by the enzyme, FAM dyes were released to generate fluorescence signals. Each step of the motor strand walking on the GNP track, more and more FAM dyes were released, realizing a signal amplification process. This assay had an LOD of 8.2×10^3 exosomes/mL and a linear range from 2×10^4 to 2×10^9 particles/mL. This assay detected higher exosomal CD63 levels in serum samples from breast cancer patients ($n=10$) than normal controls ($n=10$).

Gao *et al.*³⁶ developed a dual signal amplification method to detect exosomal CD63 from HepG2 liver cancer cells. This dual signal amplification was realized by coupling a catalytic hairpin DNA cascade reaction (HDCR) with a DNA dendrimer assembly strategy. In this assay, magnetic beads were conjugated with CD63 aptamers and DNA block probes (partially hybridized to CD63 aptamers). The

capture of exosomes expressing CD63 released the DNA block probes, which hybridized with hairpin probes HP1 on gold nanoparticles (AuNP). Hairpin probes HP2 were then added to replace the DNA block probes and initiate the HDCR to achieve the first signal amplification. Part of the HP1 sequence was designed to be complementary to fluorescent, sticky-ended and Y-shaped DNAs, and therefore, HP1 probes also served as an anchor for the self-assembly of Y-shaped DNAs to form DNA dendrimers on AuNP, which provided the second signal amplification. The AuNP-HP1-HP2-dendrimer complexes were collected and the fluorescence intensity was measured to quantify the expression of exosomal CD63. This assay detected CD63 in HepG2 cell-derived exosomes with an LOD of 1.16×10^6 exosomes/mL and a linear range from 1.75×10^6 to 7×10^9 exosomes/mL.

Nanostructured materials were employed in microfluidic devices to improve the interaction between exosomes and capture probes and thus achieve better sensing performances. Zhang *et al.*³⁷ developed a nano-interfaced microfluidic exosome (nano-IMEX) biosensor for ovarian cancer diagnosis. Y-shaped polydimethylsiloxane (PDMS) microposts were bonded to a glass substrate to prepare the microfluidic device. Then graphene oxide (GO) and polydopamine (PDA) solutions were sequentially flowed through the microfluidic device to create a nanostructured coating on the glass and PDMS surfaces. Antibodies were immobilized onto the surface for immuno-capture of exosomes. The expression of exosomal protein targets was measured by fluorogenic ELISA. The LOD of the nano-IMEX biosensor was $\sim 5 \times 10^4$ exosomes/mL with a 4-log dynamic range. The sensitivity of the nano-IMEX biosensor was 1000-fold higher than that of conventional ELISA. Using exosomal CD9, CD81, and EpCAM as biomarkers, the nano-IMEX biosensor successfully distinguished ovarian cancer patients ($n=7$) from healthy controls ($n=5$).

Zhang *et al.*³⁸ developed a 3D-nanopatterned herringbone (nano-HB) microfluidic device for ovarian cancer diagnosis. A multiscale integration by designed self-assembly (MINDS) approach was used to create herringbone structures using 960 nm silica colloids in the microfluidic device (Figure 7). The porous structures assisted in draining the boundary fluid, reducing near-surface hydrodynamic resistance and thus increasing interaction between exosomes and the surface. The porous structures also offered a large surface area for antibody immobilization, which enhanced the exosome capture efficiency. The expression of exosomal proteins

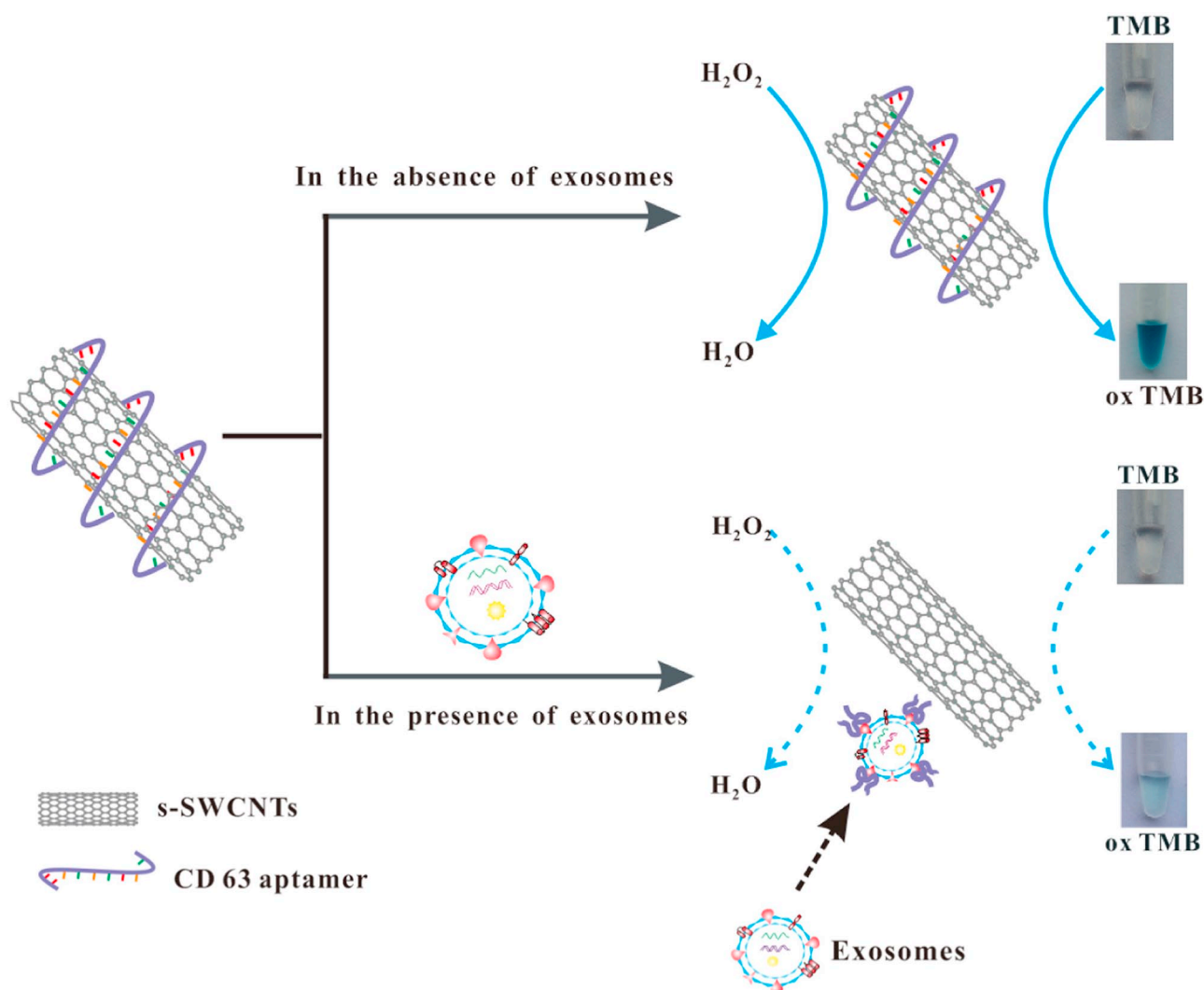


Figure 8. Sensing mechanism of the colorimetric aptasensor for exosomal CD63 detection. CD63 aptamers adsorbed on SWCNTs improved the peroxidase activity of SWCNTs, which catalyzed the oxidation of 3,3',5,5'-tetramethylbenzidine (TMB) in the presence of H_2O_2 and changed the solution from colorless to deep blue. In the presence of exosomes, CD63 aptamers bound to exosomes and were released from the surface of SWCNTs. This process transformed the SWCNTs into their original state, decreased catalytic activity, and changed the color of the solution from deep blue to moderate blue. (Reprinted from Xia *et al.*³⁹ ©2017 Elsevier B.V.) (A color version of this figure is available in the online journal.)

was quantified by fluorogenic ELISA. The nano-HB assay detected significantly higher levels of exosomal CD24, EpCAM and FR α in plasma samples from ovarian cancer patients ($n=20$) than normal controls ($n=10$), suggesting its potential utility in ovarian cancer diagnosis. The nano-HB assay had an LOD of 10^4 exosomes/mL and a linear range of 10^5 – 10^9 exosomes/mL.

Colorimetric biosensors for exosomal protein detection

A colorimetric aptasensor was developed to quantify exosomal CD63 through the use of single-walled carbon nanotubes (SWCNTs) combined with CD63 aptamers.³⁹ As shown in Figure 8, CD63 aptamers were adsorbed on the surface of SWCNTs and helped improve the peroxidase activity of SWCNTs, which can then catalyze the oxidation of 3,3',5,5'-tetramethylbenzidine (TMB) in the presence of H_2O_2 and ultimately change the solution from colorless to blue. When exosomes were present, CD63 aptamers were bound with

exosomes and desorbed from SWCNTs. This process transformed the SWCNTs into their original state, thus decreasing catalytic activity as well as the overall color change of the solution from deep blue to moderate blue. This color change was quantified by UV-visible spectrometry and converted to exosomal CD63 expression. The LOD of this colorimetric aptasensor was 5.2×10^8 exosomes/mL (10-fold higher than ELISA), and the linear range was approximately between 1.84×10^9 and 2.21×10^{10} exosomes/mL. The colorimetric aptasensor involved a simplified experimental process, avoided the use of labeling to detect the exosomal proteins, and thus provided a user-friendly and low-cost assay in resource-limited settings.

Electrical/electrochemical-based biosensors for exosomal protein detection

Electrochemical aptasensors were developed to employ aptamers for exosome detection. Wang *et al.*⁴⁰ designed a portable DNA nanotetrahedron (NTH)-assisted aptasensor

to detect HepG2 hepatocarcinoma cell-derived exosomes. DNA NTH containing LZH8 aptamers was attached to the surface of gold electrodes. The capture of exosomes induced a significant decrease in current signals from the ferricyanide–ferrocyanide redox couple. The DNA NTH precisely controlled the spatial orientation of the LZH8 aptamers on the electrode surface, allowing sensitive exosome detection with an LOD of 2.09×10^4 exosomes/mL and a linear range of 10^5 – 10^{12} exosomes/mL. Dong *et al.*⁴¹ developed an aptasensor with signal amplification capability for sensitive detection of exosomal prostate-specific membrane antigen (PSMA). On magnetic beads, PSMA aptamer-messenger DNA (mDNA) complexes were conjugated. When PSMA aptamers captured exosomes, mDNAs were released. Magnetic separation was then performed to separate exosomes from mDNAs. The amount of released mDNAs, which was correlated with the expression of exosomal PSMA, was measured using an electrochemical method. Briefly, mDNAs hybridized with DNA probes on a gold surface. Then the Exo III enzyme was added to initiate cyclic enzymatic amplification of electrochemical signals, allowing the sensitive detection of the levels of mDNAs. With LNCaP cell-derived exosomes, this aptasensor showed an LOD of 7×10^4 exosomes/mL and a linear range of 10^6 – 1.2×10^8 exosomes/mL.

Field effect transistor (FET) biosensors as a label free sensing approach have been developed to quantify exosomal protein expression. Yu *et al.*⁴² developed a reduced graphene oxide (RGO)-based FET biosensor and demonstrated its potential application in prostate cancer diagnosis. The RGO FET biosensor was fabricated by sequentially depositing RGO, 1-Pyrenebutanoic acid succinimidylester (PASE) and CD63 antibodies on a SiO₂/Si substrate. After exosomes were captured by CD63 antibodies, the negative charges of exosomes led to the left shift of the Dirac point, allowing the quantification of exosomal CD63 expression. The RGO FET biosensor had the LOD of 3.3×10^4 exosomes/mL and the linear range of 3.3×10^4 – 3.3×10^9 exosomes/mL. It detected significantly higher levels of exosomal CD63 in serum samples from prostate cancer patients ($n=6$) than normal controls ($n=8$). A similar graphene FET biosensor was reported by Kwong Hong Tsang *et al.*⁴³ to quantify CD63 expression in exosomes isolated from healthy donors' plasma samples. The LOD of graphene FET biosensor was 0.1 $\mu\text{g/mL}$, corresponding to $\sim 5 \times 10^6$ exosomes/mL.

Metal-organic frameworks (MOFs) have emerged as attractive nanomaterials in biosensing applications because of their unique properties, such as high surface area, high porosity, diverse surface functionalization, and biocompatible. Cao *et al.*⁴⁴ developed a ZIF-8-based electrochemical biosensor for breast cancer diagnosis (Figure 9). Magnetic beads conjugated with CD63 antibodies were first used to capture exosomes. Then PD-L1 antibodies modified capture probes were added to bind to exosomes expressing PD-L1. The capture probes then served as the primers to initiate hyperbranched rolling circle amplification, which lowered the pH and led to the disassembly of PV@HRP@ZIF-8 MOFs and the release of HRP enzyme. The HRP enzyme generated electrochemical signals which were converted to the expression of exosomal PD-L1. This ZIF-8-based electrochemical

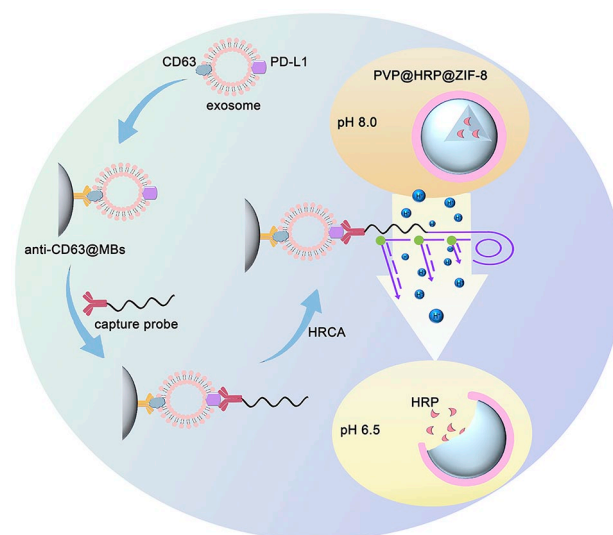


Figure 9. Schematic of detection of exosomal PD-L1 using a ZIF-8 MOF-based electrochemical biosensor for breast cancer diagnosis. Magnetic beads conjugated with CD63 antibodies were first used to capture exosomes. Then PD-L1 antibodies modified capture probes were added to bind to exosomes expressing PD-L1. The capture probes then served as the primers to initiate hyperbranched rolling circle amplification, which lowered the pH and led to the disassembly of PV@HRP@ZIF-8 MOFs and the release of HRP enzyme. The HRP enzyme generated electrochemical signals which were correlated with the expression of exosomal PD-L1. (Reprinted with permission from Cao *et al.*⁴⁴ ©2020 Elsevier B.V.) (A color version of this figure is available in the online journal.)

biosensor showed an LOD of 334 exosomes/mL and a linear range of 10^3 – 10^{10} exosomes/mL. It detected higher exosomal PD-L1 levels in exosomes from MDA-MB-231 and MCF-7 cells than those from L02 cells. The expression of exosomal PD-L1 was also higher in serum samples from breast cancer patients ($n=15$) than normal controls ($n=6$). Sun *et al.*⁴⁵ developed an electrochemical biosensor using Zr-based MOFs, that is, UiO-66 to detect exosomal EGFR and EGFRvIII for glioblastoma diagnosis. Exosomes expressing EGFR or EGFRvIII were first captured by peptide ligands tethered to an Au electrode. Then UiO-66 loaded with methylene blue molecules (MB@UiO-66) was added to bind with exosomes through the formation of Zr-O-P bonds, which produced electrochemical signals for sensitive detection of exosomal EGFR and EGFRvIII. This Zr-MOF-based electrochemical biosensor had an LOD of 7.83×10^6 exosomes/mL and a linear range of 9.5×10^6 – 1.9×10^{10} exosomes/mL. It detected significantly higher levels of exosomal EGFR and EGFRvIII in serum samples from glioblastoma patients ($n=8$) than normal controls ($n=8$).

Plasmonics-based biosensors for exosomal protein detection

Im *et al.*⁴⁶ developed a nanoplasmonic exosome (nPLEX) biosensor that consisted of arrays of periodic nanohole patterns in the metal film (Figure 10). The surface of the nPLEX biosensor was modified with antibodies. The binding of exosomal proteins with antibodies induced the spectral shifts or intensity changes of the laser light, which were recorded and converted to the expression of exosomal proteins. The LOD of the nPLEX assay was $\sim 3,000$ exosomes, which was 10^4 -fold

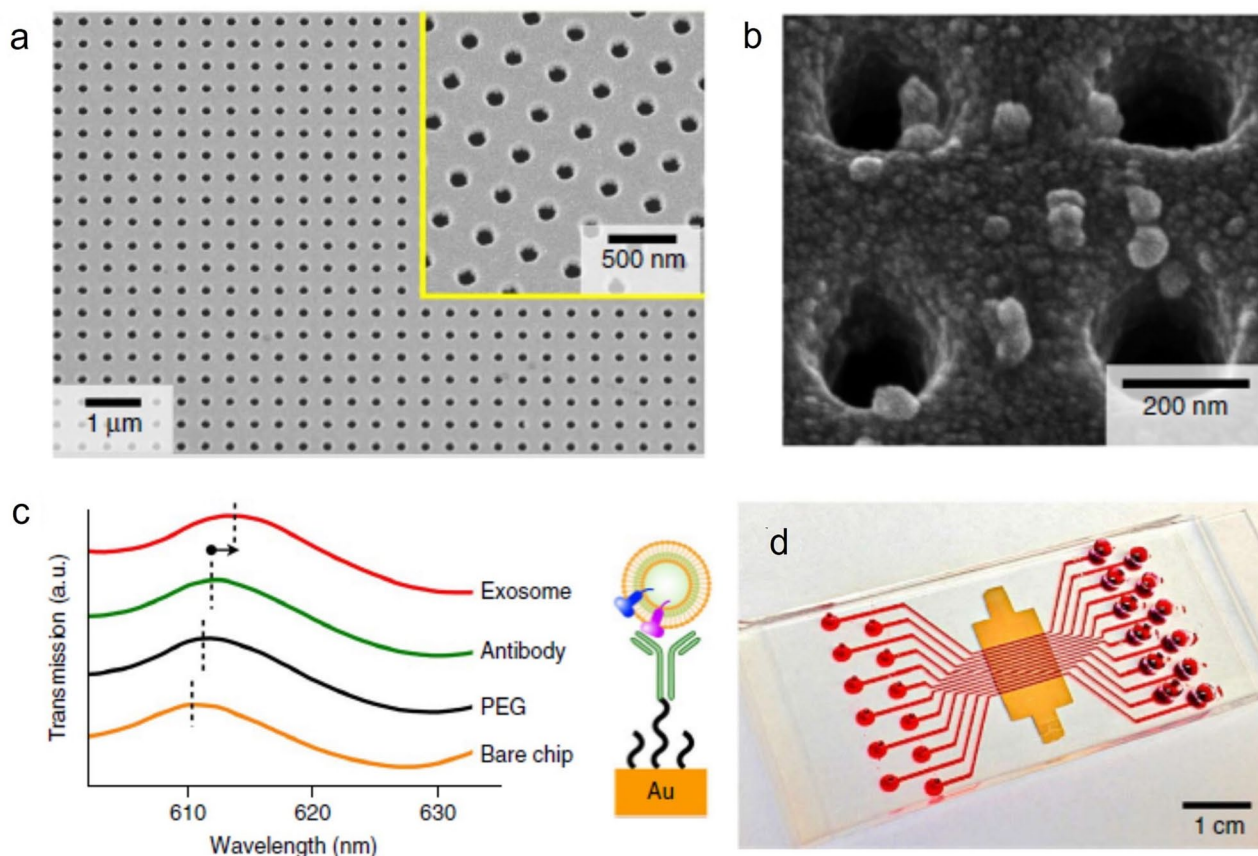


Figure 10. Design and sensing mechanism of nPLEX biosensor. (a) An SEM image of periodic nanoholes in the nPLEX biosensor. (b) An SEM image of exosomes captured by antibodies modified on the surface of the nPLEX biosensor. (c) Representative responses (transmission spectra shifts and intensity increases) to the binding of PEG, antibody, and exosomes on the nPLEX biochip. (d) A picture of nPLEX biochip integrated with a multichannel microfluidic cell. (Reprinted from Im *et al.*⁴⁶ ©2014 Nature America, Inc.) (A color version of this figure is available in the online journal.)

higher than western blot and 10^2 -fold higher than ELISA. By integrating in a multichannel microfluidic device, the nPLEX biosensor allowed multiplex detection of exosomal proteins. Using exosomal EpCAM and CD24 as the biomarkers, the nPLEX biosensor not only distinguished ovarian cancer patients ($n=20$) from non-cancerous cirrhosis controls ($n=10$) with 97% accuracy, but also predicted the responses to chemotherapy, demonstrating its potential application in ovarian cancer diagnosis and treatment response evaluation.

The nanofabrication of nanoplasmonic devices is an expensive and low-throughput process. To address these challenges, Wu *et al.*⁹ developed an exosome-templated nanoplasmonic assay termed the templated plasmonics for exosomes (TPEX) assay, which did not require the fabrication of nanoplasmonic devices. In the TPEX assay, exosomes were first labeled with fluorescent dye A647 modified aptamers that target exosomal protein biomarkers. Then the exosomes were labeled with gold nanoparticles, which served as the seeds for in situ growth of gold nanoshells on the outside of exosomes in the presence of gold salt. The exosome-templated gold nanoshells showed a red shift of the plasmonic resonance peak from 540 nm to 750 nm, which effectively quenched the fluorescent signals of the A647 aptamers and allowed the detection of exosomal proteins. To enable the point-of-care testing, the TPEX assay was integrated into a microfluidic device and the fluorescence signals were

detected by a smartphone-based optical detector. The TPEX assay only required 1 μ L sample and 15 min to complete. It had an LOD of 1500 exosomes and a linear range of 10^5 – 10^7 exosomes/mL. The sensitivity of the TPEX assay was >1000-fold higher than ELISA. The clinical utility of the TPEX assay was demonstrated in detecting exosomal CD63, CD24, EpCAM, and MUC1 in ascites from colorectal cancer patients ($n=12$) and gastric cancer patients ($n=8$). The combination of all four exosomal biomarkers provided an accuracy of 97% in predicting both the clinical outcome and patient survival.

SERS-based biosensors for exosomal protein detection

SERS immunoassays have been developed for exosomal protein characterization. Zong *et al.*⁴⁷ first conjugated CD63 antibodies on the surface of silica-coated magnetic nanobeads. Then, SERS nanoprobe were prepared by coating Au@Ag nanorods with SERS reporters (DTNB, 5,5'-dithiobis (2-nitrobenzoic acid)), silica shells, and HER2 antibodies. When exosomes were present, the SERS probe-exosome-magnetic nanobead immunocomplexes were formed. After magnetic separation, SERS was used to analyze the expression of exosomal HER2. This assay detected a 3.8-fold higher signal from exosomes derived from SKBR3 breast cancer cells than those from MRC5 normal lung fibroblasts. The

LOD of this assay was ~1200 exosomes. Pang *et al.*⁴⁸ first enriched the exosomes with Fe₃O₄@TiO₂ nanoparticles and then used PD-L1 antibody-labeled SERS nanoprobe (Au@Ag@Mercaptobenzoic acid [MBA]) to quantify the expression of exosomal PD-L1. The LOD of this assay was 1000 exosomes/mL. Significantly higher levels of exosomal PD-L1 were observed in serum samples from lung cancer patients ($n=17$) than normal controls ($n=12$).

Multiplex and high-throughput SERS assays were developed to improve sensing efficiency. Zhang *et al.*⁴⁹ developed a multiplexed SERS assay. GPC1 antibodies, EpCAM antibodies and CD44V6 antibodies were conjugated on three SERS nanoprobe (Au@DTNB, Au@MBA and Au@TFMBA(2,3,5,6-Tetrafluoro-4-mecaptobenzonic acid)). After the labeling of exosomes with three SERS nanoprobe, magnetic beads modified with CD63 antibodies were added to isolate exosomes for SERS characterization. The multiplex sensing capability was demonstrated by the simultaneous detection of GPC1, EpCAM and CD44V6 in exosomes from Panc-1 pancreatic cancer cells, SW480 colorectal cancer cells and C3 bladder cancer cells. This assay had an LOD of 2.3×10^6 exosomes/mL. Kwizera *et al.*⁵⁰ developed an antibody microarray-based, high throughput SERS assay. A 17×5 antibody microarray was fabricated on a gold-coated glass slide. Exosomes were applied to allow the antibodies to capture exosomes expressing target proteins. Then gold nanorods coated with cetyltrimethylammonium bromide (CTAB) and Raman reporter QSY21 were added to bind with exosomes through electrostatic interaction between positively charged gold nanorods and negatively charged exosomes. SERS signals were detected to quantify the expression of exosomal proteins. This high throughput assay analyzed more than 80 exosome samples on a single device within 2h with an LOD of 2×10^6 exosomes/mL. Exosomal HER2, EpCAM, CD44, CD81, CD63, and CD9 were detected in plasma samples from breast cancer patients ($n=10$) and normal controls ($n=5$). Among these markers, exosomal HER2 and EpCAM detected breast cancer with 100% accuracy.

SERS aptasensors have been developed to use aptamers to replace antibodies in SERS immunoassay. Fan *et al.*¹⁰ reported an SERS-EpCAM aptasensor to detect exosomal EpCAM for lung cancer diagnosis. In this assay, EpCAM aptamers were first used to capture exosomes expressing EpCAM. Polylysine-based SERS reporters were then attached to the EpCAM aptamer-exosome complexes through click reaction. Finally, gold nanostars were added to serve as SERS substrates for detection. By controlling the length of polylysine, the number of SERS reporters could be adjusted, enabling programmable signal amplification. With optimized polylysine length, the LOD of this aptasensor was 2.4×10^3 exosomes/mL, which was >500-fold higher than that of ELISA (1.3×10^6 exosomes/mL). Significantly higher exosomal EpCAM expression was observed in plasma samples from lung cancer patients ($n=3$) than normal controls ($n=3$). Zhu *et al.*⁵¹ developed a SERS aptasensor based on a hydrophobic assembled nanoacorn (HANA) platform. As shown in Figure 11, a thin gold film was first deposited on polystyrene nanosphere arrays to serve as the hydrophobic plasmonic substrate. Then ultrathin, hydrophilic sensing patches

were generated by layer-by-layer assembly of polyacrylic acid/Rhodamine 6G, poly(allylamine hydrochloride) and aptamers onto the surfaces of the plasmonic substrate. SERS nanoprobe (i.e. Au@Ag nanocubes) were then added for exosomal protein detection. In the absence of exosomes, the negatively charged Au@Ag nanocubes were not able to bind to the sensing patches because of strong electrical repulsion. In the presence of exosomes, aptamers bound with exosomes and dissociated from the plasmonic substrate, which allowed the assembly of Au@Ag nanocubes on the sensing patches, forming a nanoparticle-on-mirror (NPOM) array. This NPOM array greatly enhanced the SERS signals of Rhodamine 6G, enabling sensitive detection of exosomal proteins. The LOD of the HANA assay was 50 exosomes/mL. Using exosomal CD63, EpCAM, and HER2 as the combined biomarkers, the HANA assay distinguished breast cancer patients ($n=7$) from normal controls ($n=7$) with 100% accuracy, demonstrating its feasibility in breast cancer diagnosis.

Novel SERS probes were developed to improve sensing performance. Zhang *et al.*⁵² prepared a new SERS probe by first mixing negatively charged triangular pyramid DNA (TP DNA) with positively charged gold nanoparticles to prepare TP-AuNP complexes and then decorating the TP-AuNP complexes with DNTB for SERS sensing. The potential application of the TP-AuNP-DNTB probe was demonstrated in detecting exosomal EpCAM for breast cancer diagnosis. Magnetic beads were conjugated with EpCAM aptamers to capture exosomes expressing EpCAM. The TP-AuNP-DNTB probes were conjugated with cholesterol modified linker DNA to allow binding with exosomes through the hydrophobic interaction between cholesterol and the exosome lipid membrane. The magnetic bead-exosome-TP-AuNP-DNTB complexes generated strong SERS signals for quantitative detection of exosomal EpCAM. This TP-AuNP-DNTB based SERS aptasensor had an LOD of 1.1×10^5 exosomes/mL and a linear range of 10^6 – 10^{10} exosomes/mL. This assay detected significantly higher expression of exosomal EpCAM in plasma samples of breast cancer patients ($n=3$) than normal controls ($n=3$). Ning *et al.*⁵³ reported unique bimetallic SERS probes, that is, gold-silver-silver core-shell-shell nanotrepangs (GSSNTs) encoded with three Raman dyes (2-Mpy, 4-ATP or NTP) for multiplex detection of exosomal proteins. GSSNTs were conjugated with linker DNAs partially complementary to PSMA, HER2 and AFP aptamers. The GSSNTs were then mixed with magnetic beads modified with PSMA, HER2 and AFP aptamers to form GSSNT-magnetic bead complexes. When exosomes were added, exosomes were captured by the aptamers, which caused the release of GSSNT probes from magnetic beads and thus the attenuation of SERS signals. The SERS signal reduction was correlated with the expression of exosomal proteins. The LOD of this assay was 2.6×10^4 , 7.2×10^4 and 3.5×10^4 exosomes/mL for detecting exosomal PSMA, HER2, and AFP from LNCaP prostate cancer cells, SKBR3 breast cancer cells, and HepG2 liver cancer cells, respectively. This assay also detected exosomal PSMA, HER2, and AFP in serum samples from patients with prostate cancer ($n=1$), breast cancer ($n=1$), and hepatocellular carcinoma ($n=1$).

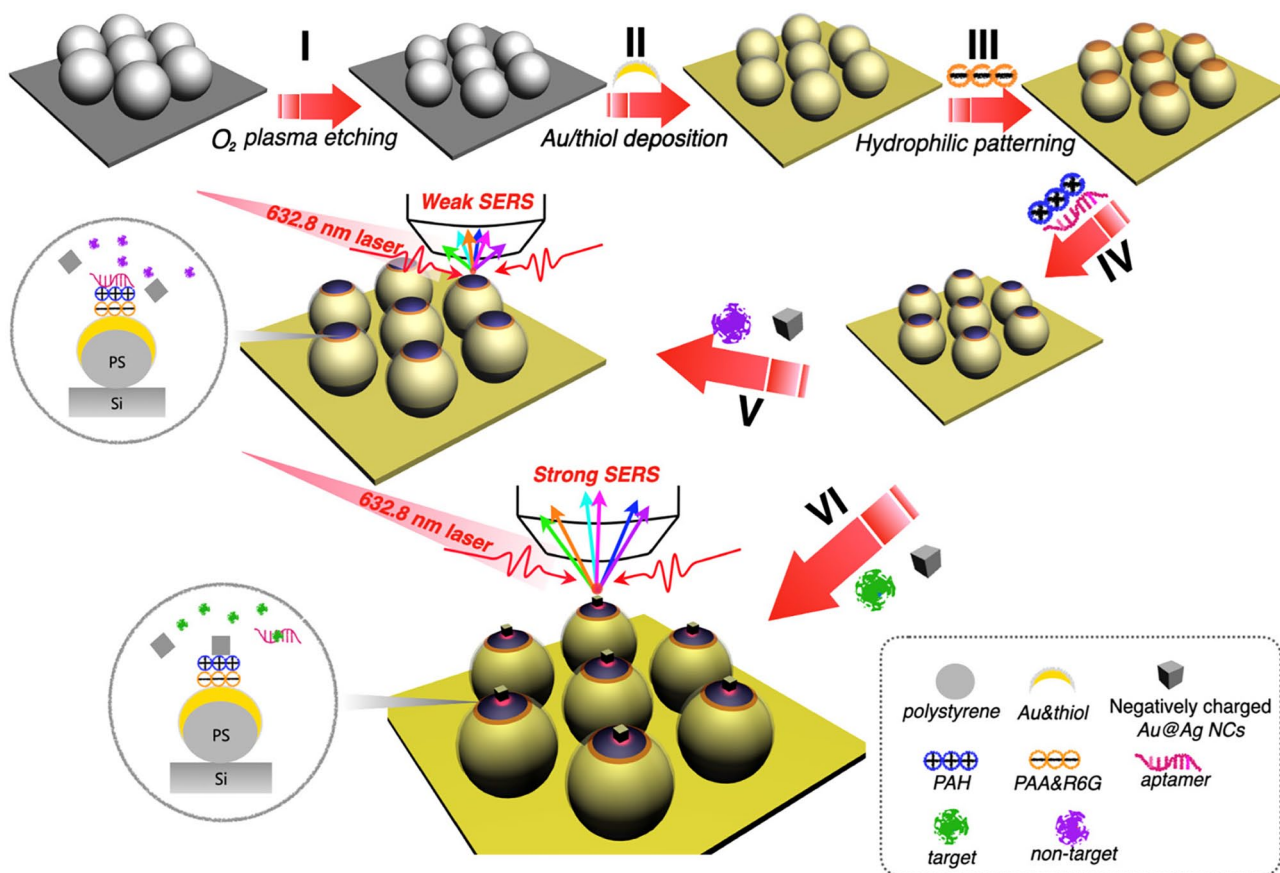


Figure 11. Sensing mechanism of SERS aptasensor based on a hydrophobic assembled nanoacorn (HANA) platform. The HANA platform was prepared by depositing a thin gold film on polystyrene nanosphere arrays, followed by layer-by-layer assembly of polyacrylic acid (PAA)/Rhodamine 6G (R6G), poly(allylamine hydrochloride) (PAH) and aptamers onto the surfaces of the plasmonic substrate to form ultrathin, hydrophilic sensing patches. SERS nanoprobes (Au@Ag nanocubes) were then added for exosomal protein detection. In the absence of exosomes, the negatively charged Au@Ag nanocubes were not able to bind on the sensing patches because of strong electrical repulsion. In the presence of exosomes, aptamers bound with exosomes and dissociated from the plasmonic substrate, which allowed the assembly of Au@Ag nanocubes on the sensing patches, forming a nanoparticle-on-mirror (NPoM) array. This NPoM array greatly enhanced SERS signals of Rhodamine 6G, enabling sensitive detection of exosomal proteins. (Reprinted from Zhu *et al.*⁵¹ ©2020 American Chemical Society.) (A color version of this figure is available in the online journal.)

ICP-MS and photothermal-based biosensors for exosomal protein detection

Zhang *et al.*⁵⁴ developed an ICP-MS and photothermal dual-readout assay to detect exosomal GPC1 for pancreatic cancer diagnosis (Figure 12). Magnetic beads conjugated with CD63 antibodies were first used to capture exosomes. Then exosomes expressing GPC1 were labeled by GPC1 antibodies conjugated with alkaline phosphatase (ALP). L-ascorbic acid 2-phosphate (AAP) and $\text{Fe}_3\text{O}_4@\text{MnO}_2$ nanoflowers were added to initiate the hydrolysis of AAP by ALP and the etching of $\text{Fe}_3\text{O}_4@\text{MnO}_2$ nanoflowers to release Mn^{2+} . After magnetic separation, the level of Mn^{2+} in the supernatant was quantified by ICP-MS. The reduced $\text{Fe}_3\text{O}_4@\text{MnO}_2$ nanoflowers were reacted with dopamine to generate polydopamine nanoparticles, which were irradiated by a near-infrared laser to generate photothermal signals. The readouts from ICP-MS and photothermal analyses were converted to the expression of exosomal GPC1. The LOD of ICP-MS assay was 19.1 exosomes/mL and the linear range was 45– 4.5×10^6 exosomes/mL. The photothermal assay was less sensitive than the ICP-MS assay, with a linear

range of 2.5×10^8 – 4.5×10^9 exosomes/mL. The ICP-MS assay detected significantly higher levels of exosomal GPC1 in serum samples from pancreatic cancer patients ($n=9$) than normal controls ($n=6$). However, the photothermal assay was only able to distinguish normal controls from patients with high exosomal GPC1 expression but not those with low exosomal GPC1 expression, suggesting that the photothermal assay may serve as a pre-screening tool.

Conclusions and perspectives

Exosomes, the intercellular messengers released by cells, stably exist in all types of body fluids in large quantities. They transport various cargoes, including DNAs, RNAs, proteins, and lipids, between cells for intercellular communication. Exosomes play important roles in cancer growth, angiogenesis, immune modulation, metastasis, and drug resistance, and therefore, they represent a new class of circulating biomarker for cancer screening, diagnosis, treatment response monitoring, and prognosis. Current characterization techniques, such as ELISA and qRT-PCR, are limited by

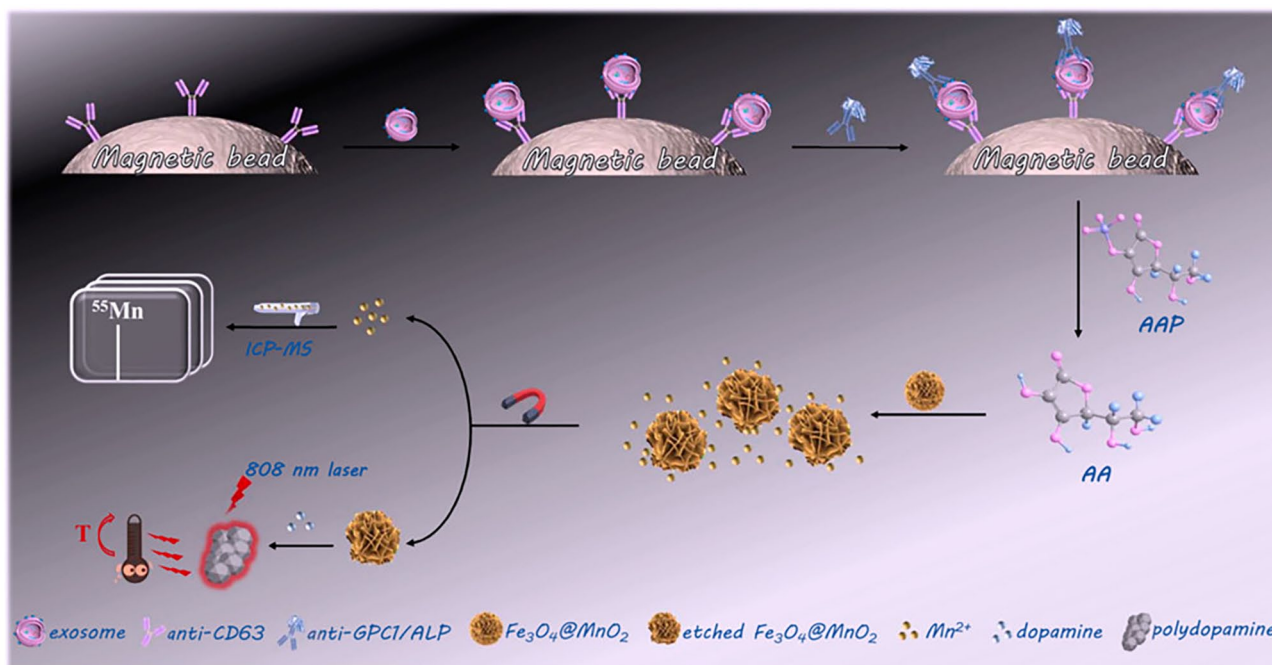


Figure 12. Sensing mechanism of ICP-MS and photothermal dual-readout assay for the detection of exosomal GPC1 for pancreatic cancer diagnosis. Magnetic beads modified with CD63 antibodies captured exosomes. Then exosomes expressing GPC1 were labeled by GPC1 antibodies conjugated with alkaline phosphatase (ALP). L-ascorbic acid 2-phosphate (AAP) and $\text{Fe}_3\text{O}_4@\text{MnO}_2$ nanoflowers were added to initiate the hydrolysis of AAP by ALP and the etching of $\text{Fe}_3\text{O}_4@\text{MnO}_2$ nanoflowers to release Mn^{2+} . After magnetic separation, the level of Mn^{2+} in supernatant was quantified by ICP-MS. The reduced $\text{Fe}_3\text{O}_4@\text{MnO}_2$ nanoflowers were reacted with dopamine to generate polydopamine nanoparticles, which were irradiated by a near-infrared laser to generate photothermal signals. (Reprinted from Zhang *et al.*⁵⁴ ©2021 American Chemical Society.) (A color version of this figure is available in the online journal.)

low sensitivity and tedious and time-consuming procedures, and thus they are not suitable for clinical settings, especially for point-of-care testing. Many biosensors have been developed recently to offer highly sensitive, simple, fast, and high-throughput analysis of exosomes. Although still in an early stage, emerging evidence has shown the potential applications of these biosensors in cancer diagnosis.

In the future, continuous development and improvement are still required to develop exosome-based biosensors into robust liquid biopsy tests for cancer. First, the detection sensitivity, specificity, and reproducibility of the biosensors need to be further improved to be able to handle complex biological samples, such as blood, urine, ascites fluids, and saliva. Many other components in the biological samples, such as cells, proteins, nucleic acids and lipids, may introduce significant interference to the exosome detection. The biosensors should be able to selectively capture tumor-derived exosomes from the samples and offer accurate measurements of exosomal biomarkers. Second, the diagnostic values of these biosensors need to be validated in large cohorts of patients to evaluate their reliability and justify their clinical utility. Currently, potential applications of many biosensors in cancer diagnosis are only demonstrated using small numbers of patients. Large scale validations with consideration of patient characteristics, such as age, gender, race, cancer stages, and subtypes, are urgently needed. Finally, the biosensors should embrace user-friendly and cost-effective designs to promote clinical translation and facilitate the commercialization. Many biosensors require costly fabrication processes, expensive supporting equipment, and intensive

user training, which may greatly limit their adaptability to clinical settings. Biosensors that provide accurate, simple, fast, and cheap detection of exosomes are desired.

In summary, exosome-based, nanotechnology-enabled biosensors are exciting liquid biopsy tests that may be used as complementary or companion tests in cancer screening, diagnosis, and prognosis. They may also assist in personalized medical decision-making and monitoring treatment responses. Although the development of exosome-based biosensors is still in a very early stage, rapid and significant progress made in recent years has indicated their great potential and promising future in cancer care.

AUTHORS' CONTRIBUTIONS

YW conceived the concept and supervised the study. CCH and YW performed literature search and wrote the manuscript.


DECLARATION OF CONFLICTING INTERESTS

The author(s) declared no potential conflicts of interest with respect to the research, authorship, and/or publication of this article.

FUNDING

The author(s) disclosed receipt of the following financial support for the research, authorship, and/or publication of this article: This work was supported by the National Cancer Institute of the National Institutes of Health (grant number R21CA235305). The content is solely the responsibility of the authors and does not necessarily represent the official views of the National Institutes of Health.

ORCID IDS

Chang-Chieh Hsu  <https://orcid.org/0000-0002-4507-3268>Yun Wu  <https://orcid.org/0000-0002-6926-777X>

REFERENCES

- Ignatiadis M, Sledge GW, Jeffrey SS. Liquid biopsy enters the clinic—implementation issues and future challenges. *Nat Rev Clin Oncol* 2021; **18**:297–312
- Siravegna G, Marsoni S, Siena S, Bardelli A. Integrating liquid biopsies into the management of cancer. *Nat Rev Clin Oncol* 2017; **14**:531–48
- Kalluri R, LeBleu VS. The biology, function, and biomedical applications of exosomes. *Science* 2020; **367**:eaau6977
- Möller A, Lobb RJ. The evolving translational potential of small extracellular vesicles in cancer. *Nat Rev Cancer* 2020; **20**:697–709
- LeBleu VS, Kalluri R. Exosomes as a multicomponent biomarker platform in cancer. *Trends Cancer* 2020; **6**:767–74
- Zhou B, Xu K, Zheng X, Chen T, Wang J, Song Y, Shao Y, Zheng S. Application of exosomes as liquid biopsy in clinical diagnosis. *Signal Trans Target Therapy* 2020; **5**:1–14
- Hu J, Sheng Y, Kwak KJ, Shi J, Yu B, Lee LJ. A signal-amplifiable biochip quantifies extracellular vesicle-associated RNAs for early cancer detection. *Nat Commun* 2017; **8**:1–11
- Yang Y, Kannisto E, Yu G, Reid ME, Patnaik SK, Wu Y. An immuno-biochip selectively captures tumor-derived exosomes and detects exosomal RNAs for cancer diagnosis. *ACS Appl Mater Interf* 2018; **10**:43375–86
- Wu X, Zhao H, Natalia A, Lim CZJ, Ho NRY, Ong CJ, Teo MCC, So JBY, Shao H. Exosome-templated nanoplasmonics for multiparametric molecular profiling. *Sci Adv* 2020; **6**:eaba2556
- Fan C, Zhao N, Cui K, Chen G, Chen Y, Wu W, Li Q, Cui Y, Li R, Xiao Z. Ultrasensitive exosome detection by modularized sers labeling for postoperative recurrence surveillance. *ACS Sensors* 2021; **6**:3234–41
- Wu Y, Kwak KJ, Agarwal K, Marras A, Wang C, Mao Y, Huang X, Ma J, Yu B, Lee R. Detection of extracellular RNAs in cancer and viral infection via tethered cationic lipoplex nanoparticles containing molecular beacons. *Anal Chem* 2013; **85**:11265–74
- Liu C, Kannisto E, Yu G, Yang Y, Reid ME, Patnaik SK, Wu Y. Non-invasive detection of exosomal MicroRNAs via tethered cationic lipoplex nanoparticles (tCLN) biochip for lung cancer early detection. *Front Genet* 2020; **11**:258
- Lee LJ, Yang Z, Rahman M, Ma J, Kwak KJ, McElroy J, Shilo K, Goparaju C, Yu L, Rom W. Extracellular mRNA detected by tethered lipoplex nanoparticle biochip for lung adenocarcinoma detection. *Am J Resp Critic Care Med* 2016; **193**:1431–3
- Wang X, Kwak KJ, Yang Z, Zhang A, Zhang X, Sullivan R, Lin D, Lee RL, Castro C, Ghoshal K, Schmidt C, Lee LJ. Extracellular mRNA detected by molecular beacons in tethered lipoplex nanoparticles for diagnosis of human hepatocellular carcinoma. *PLoS ONE* 2018; **13**:e0198552
- Pu X, Ding G, Wu M, Zhou S, Jia S, Cao L. Elevated expression of exosomal microRNA-21 as a potential biomarker for the early diagnosis of pancreatic cancer using a tethered cationic lipoplex nanoparticle biochip. *Oncol Lett* 2020; **19**:2062–70
- Zhou J, Wu Z, Hu J, Yang D, Chen X, Wang Q, Liu J, Dou M, Peng W, Wu Y, Wang W, Xie C, Wang M, Song Y, Zeng H, Bai C. High-throughput single-EV liquid biopsy: rapid, simultaneous, and multiplexed detection of nucleic acids, proteins, and their combinations. *Sci Adv* 2020; **6**:eabc1204
- Yang Y, Kannisto E, Patnaik SK, Reid ME, Li L, Wu Y. Ultrafast detection of exosomal mas via cationic lipoplex nanoparticles in a micromixer biochip for cancer diagnosis. *ACS Appl Nano Mater* 2021; **4**:2806–19
- He D, Wang H, Ho SL, Chan HN, Hai L, He X, Wang K, Li HW. Total internal reflection-based single-vesicle in situ quantitative and stoichiometric analysis of tumor-derived exosomal microRNAs for diagnosis and treatment monitoring. *Theranostics* 2019; **9**:4494–507
- Zhao J, Liu C, Li Y, Ma Y, Deng J, Li L, Sun J. Thermophoretic detection of exosomal microRNAs by nanoflares. *J Am Chem Soc* 2020; **142**:4996–5001
- Taller D, Richards K, Slouka Z, Senapati S, Hill R, Go DB, Chang H-C. On-chip surface acoustic wave lysis and ion-exchange nanomembrane detection of exosomal RNA for pancreatic cancer study and diagnosis. *Lab Chip* 2015; **15**:1656–66
- Liu N, Lu H, Liu L, Ni W, Yao Q, Zhang G-J, Yang F. Ultrasensitive exosomal microRNA detection with a supercharged DNA framework nanolabel. *Anal Chem* 2021; **93**:5917–23
- Zhang J, Wang L-L, Hou M-F, Xia Y-K, He W-H, Yan A, Weng Y-P, Zeng L-P, Chen J-H. A ratiometric electrochemical biosensor for the exosomal microRNAs detection based on bipedal DNA walkers propelled by locked nucleic acid modified toehold mediate strand displacement reaction. *Biosens Bioelectron* 2018; **102**:33–40
- Yang H, Zhao J, Dong J, Wen L, Hu Z, He C, Xu F, Huo D, Hou C. Simultaneous detection of exosomal microRNAs by nucleic acid functionalized disposable paper-based sensors. *Chem Eng J* 2022:135594
- Joshi GK, Deitz-McElyea S, Liyanage T, Lawrence K, Mali S, Sardar R, Korc M. Label-free nanoplasmonic-based short noncoding RNA sensing at attomolar concentrations allows for quantitative and highly specific assay of microRNA-10b in biological fluids and circulating exosomes. *ACS Nano* 2015; **9**:11075–89
- Wu W, Yu X, Wu J, Wu T, Fan Y, Chen W, Zhao M, Wu H, Li X, Ding S. Surface plasmon resonance imaging-based biosensor for multiplex and ultrasensitive detection of NSCLC-associated exosomal miRNAs using DNA programmed heterostructure of Au-on-Ag. *Biosens Bioelectron* 2021; **175**:112835
- Pang Y, Wang C, Lu L, Wang C, Sun Z, Xiao R. Dual-SERS biosensor for one-step detection of microRNAs in exosome and residual plasma of blood samples for diagnosing pancreatic cancer. *Biosens Bioelectron* 2019; **130**:204–13
- Lee JU, Kim WH, Lee HS, Park KH, Sim SJ. Quantitative and specific detection of exosomal miRNAs for accurate diagnosis of breast cancer using a surface-enhanced Raman scattering sensor based on plasmonic head-flocked gold nanopillars. *Small* 2019; **15**:e1804968
- Huang M, Yang J, Wang T, Song J, Xia J, Wu L, Wang W, Wu Q, Zhu Z, Song Y. Homogeneous, low-volume, efficient, and sensitive quantitation of circulating exosomal PD-L1 for cancer diagnosis and immunotherapy response prediction. *Angewandte Chemie* 2020; **132**:4830–5
- Jin D, Yang F, Zhang Y, Liu L, Zhou Y, Wang F, Zhang G-J. ExoAPP: exosome-oriented, aptamer nanoprobe-enabled surface proteins profiling and detection. *Anal Chem* 2018; **90**:14402–11
- Zhu N, Li G, Zhou J, Zhang Y, Kang K, Ying B, Yi Q, Wu Y. A light-up fluorescence resonance energy transfer magnetic aptamer-sensor for ultra-sensitive lung cancer exosome detection. *J Mater Chem B* 2021; **9**:2483–93
- Zhang J, Zhu Y, Shi J, Zhang K, Zhang Z, Zhang H. Sensitive signal amplifying a diagnostic biochip based on a biomimetic periodic nanostructure for detecting cancer exosomes. *ACS Appl Mater Interf* 2020; **12**:33473–82
- Li B, Pan W, Liu C, Guo J, Shen J, Feng J, Luo T, Situ B, Zhang Y, An T. Homogenous magneto-fluorescent nanosensor for tumor-derived exosome isolation and analysis. *ACS Sensors* 2020; **5**:2052–60
- Shi L, Ba L, Xiong Y, Peng G. A hybridization chain reaction based assay for fluorometric determination of exosomes using magnetic nanoparticles and both aptamers and antibody as recognition elements. *Microchimica Acta* 2019; **186**:16
- Huang R, He L, Li S, Liu H, Jin L, Chen Z, Zhao Y, Li Z, Deng Y, He N. A simple fluorescence aptasensor for gastric cancer exosome detection based on branched rolling circle amplification. *Nanoscale* 2020; **12**:2445–51
- Yu Y, Zhang WS, Guo Y, Peng H, Zhu M, Miao D, Su G. Engineering of exosome-triggered enzyme-powered DNA motors for highly sensitive fluorescence detection of tumor-derived exosomes. *Biosens Bioelectron* 2020; **167**:112482
- Gao M-L, He F, Yin B-C, Ye B-C. A dual signal amplification method for exosome detection based on DNA dendrimer self-assembly. *Analyst* 2019; **144**:1995–2002
- Zhang P, He M, Zeng Y. Ultrasensitive microfluidic analysis of circulating exosomes using a nanostructured graphene oxide/polydopamine coating. *Lab Chip* 2016; **16**:3033–4

38. Zhang P, Zhou X, He M, Shang Y, Tetlow AL, Godwin AK, Zeng Y. Ultrasensitive detection of circulating exosomes with a 3D-nanopatterned microfluidic chip. *Nat Biomed Eng* 2019;**3**:438–51
39. Xia Y, Liu M, Wang L, Yan A, He W, Chen M, Lan J, Xu J, Guan L, Chen J. A visible and colorimetric aptasensor based on DNA-capped single-walled carbon nanotubes for detection of exosomes. *Biosens Bioelectron* 2017;**92**:8–15
40. Wang S, Zhang L, Wan S, Cansiz S, Cui C, Liu Y, Cai R, Hong C, Teng I-T, Shi M. Aptasensor with expanded nucleotide using DNA nanotetrahedra for electrochemical detection of cancerous exosomes. *ACS Nano* 2017;**11**:3943–9
41. Dong H, Chen H, Jiang J, Zhang H, Cai C, Shen Q. Highly sensitive electrochemical detection of tumor exosomes based on aptamer recognition-induced multi-DNA release and cyclic enzymatic amplification. *Anal Chem* 2018;**90**:4507–13
42. Yu Y, Li Y-T, Jin D, Yang F, Wu D, Xiao M-M, Zhang H, Zhang Z-Y, Zhang G-J. Electrical and label-free quantification of exosomes with a reduced graphene oxide field effect transistor biosensor. *Anal Chem* 2019;**91**:10679–86
43. Kwong Hong Tsang D, Lieberthal TJ, Watts C, Dunlop IE, Ramadan S, del Rio Hernandez AE, Klein N. Chemically functionalised graphene FET biosensor for the label-free sensing of exosomes. *Sci Rep* 2019;**9**:1–10
44. Cao Y, Wang Y, Yu X, Jiang X, Li G, Zhao J. Identification of programmed death ligand-1 positive exosomes in breast cancer based on DNA amplification-responsive metal-organic frameworks. *Biosens Bioelectron* 2020;**166**:112452
45. Sun Z, Wang L, Wu S, Pan Y, Dong Y, Zhu S, Yang J, Yin Y, Li G. An electrochemical biosensor designed by using Zr-based metal-organic frameworks for the detection of glioblastoma-derived exosomes with practical application. *Anal Chem* 2020;**92**:3819–26
46. Im H, Shao H, Park YI, Peterson VM, Castro CM, Weissleder R, Lee H. Label-free detection and molecular profiling of exosomes with a nanoplasmonic sensor. *Nat Biotechnol* 2014;**32**:490–5
47. Zong S, Wang L, Chen C, Lu J, Zhu D, Zhang Y, Wang Z, Cui Y. Facile detection of tumor-derived exosomes using magnetic nanobeads and SERS nanoprobe. *Anal Meth* 2016;**8**:5001–8
48. Pang Y, Shi J, Yang X, Wang C, Sun Z, Xiao R. Personalized detection of circling exosomal PD-L1 based on Fe₃O₄@TiO₂ isolation and SERS immunoassay. *Biosens Bioelectron* 2020;**148**:111800
49. Zhang W, Jiang L, Diefenbach RJ, Campbell DH, Walsh BJ, Packer NH, Wang Y. Enabling sensitive phenotypic profiling of cancer-derived small extracellular vesicles using surface-enhanced Raman spectroscopy nanotags. *ACS Sensors* 2020;**5**:764–71
50. Kwizera EA, O'Connor R, Vinduska V, Williams M, Butch ER, Snyder SE, Chen X, Huang X. Molecular detection and analysis of exosomes using surface-enhanced Raman scattering gold nanorods and a miniaturized device. *Theranostics* 2018;**8**:2722–38
51. Zhu K, Wang Z, Zong S, Liu Y, Yang K, Li N, Wang Z, Li L, Tang H, Cui Y. Hydrophobic plasmonic nanoacorn array for a label-free and uniform SERS-based biomolecular assay. *ACS Appl Mater Interf* 2020;**12**:29917–27
52. Zhang X, Liu C, Pei Y, Song W, Zhang S. Preparation of a novel Raman probe and its application in the detection of circulating tumor cells and exosomes. *ACS Appl Mater Interf* 2019;**11**:28671–80
53. Ning C-F, Wang L, Tian Y-F, Yin B-C, Ye B-C. Multiple and sensitive SERS detection of cancer-related exosomes based on gold-silver bimetallic nanotrepangs. *Analyst* 2020;**145**:2795–804
54. Zhang Y, Wei Y, Liu P, Zhang X, Xu Z, Tan X, Chen M, Wang J. ICP-MS and photothermal dual-readout assay for ultrasensitive and point-of-care detection of pancreatic cancer exosomes. *Anal Chem* 2021;**93**:11540–6